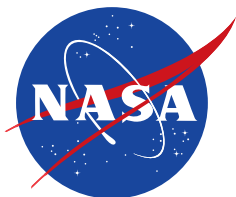


NASA/TM-2005-212874



2003 Research Engineering Annual Report

*Compiled by
Patrick C. Stoliker, Brad Flick, and Everlyn Cruciani
NASA Dryden Flight Research Center
Edwards, California*

July 2005

The NASA STI Program Office...in Profile

Since its founding, NASA has been dedicated to the advancement of aeronautics and space science. The NASA Scientific and Technical Information (STI) Program Office plays a key part in helping NASA maintain this important role.

The NASA STI Program Office is operated by Langley Research Center, the lead center for NASA's scientific and technical information. The NASA STI Program Office provides access to the NASA STI Database, the largest collection of aeronautical and space science STI in the world. The Program Office is also NASA's institutional mechanism for disseminating the results of its research and development activities. These results are published by NASA in the NASA STI Report Series, which includes the following report types:

- **TECHNICAL PUBLICATION.** Reports of completed research or a major significant phase of research that present the results of NASA programs and include extensive data or theoretical analysis. Includes compilations of significant scientific and technical data and information deemed to be of continuing reference value. NASA's counterpart of peer-reviewed formal professional papers but has less stringent limitations on manuscript length and extent of graphic presentations.
- **TECHNICAL MEMORANDUM.** Scientific and technical findings that are preliminary or of specialized interest, e.g., quick release reports, working papers, and bibliographies that contain minimal annotation. Does not contain extensive analysis.
- **CONTRACTOR REPORT.** Scientific and technical findings by NASA-sponsored contractors and grantees.
- **CONFERENCE PUBLICATION.** Collected papers from scientific and technical conferences, symposia, seminars, or other meetings sponsored or cosponsored by NASA.
- **SPECIAL PUBLICATION.** Scientific, technical, or historical information from NASA programs, projects, and missions, often concerned with subjects having substantial public interest.
- **TECHNICAL TRANSLATION.** English-language translations of foreign scientific and technical material pertinent to NASA's mission.

Specialized services that complement the STI Program Office's diverse offerings include creating custom thesauri, building customized databases, organizing and publishing research results...even providing videos.

For more information about the NASA STI Program Office, see the following:

- Access the NASA STI Program Home Page at <http://www.sti.nasa.gov>
- E-mail your question via the Internet to help@sti.nasa.gov
- Fax your question to the NASA Access Help Desk at (301) 621-0134
- Telephone the NASA Access Help Desk at (301) 621-0390
- Write to:
NASA Access Help Desk
NASA Center for AeroSpace Information
7121 Standard Drive
Hanover, MD 21076-1320

NASA/TM-2005-212874



2003 Research Engineering Annual Report

*Compiled by
Patrick C. Stoliker, Brad Flick, and Everlyn Cruciani
NASA Dryden Flight Research Center
Edwards, California*

National Aeronautics and
Space Administration

Dryden Flight Research Center
Edwards, California 93523-0273

July 2005

NOTICE

Use of trade names or names of manufacturers in this document does not constitute an official endorsement of such products or manufacturers, either expressed or implied, by the National Aeronautics and Space Administration.

Available from the following:

NASA Center for AeroSpace Information (CASI)
7121 Standard Drive
Hanover, MD 21076-1320
(301) 621-0390

National Technical Information Service (NTIS)
5285 Port Royal Road
Springfield, VA 22161-2171
(703) 487-4650

2003 Research Engineering Report

Table of Contents

<u>Title</u>	<u>First Author</u>	<u>Page</u>
Automated Aerial Refueling Hitches a Ride on AFF	Jenn Hansen	1
Real-Time Stability and Control Derivative Estimation with the F-15 #837 Aircraft	Mark Smith	3
Development and Testing of a Drogue Parachute System for X-37 ALTV/B-52H Separation	Tony Whitmore	5
Application of CONDUIT to the Active Aeroelastic Wing	Ryan Dibley	7
AAW Loads Model Verification and Validation	Michael Allen	9
Vortex-Induced Navigation Experiment (VINE)	Curtis E. Hanson	11
Evaluation of Optimal Control Allocation Methods for C-17 IFCS	Chris Regan	13
UAV Endurance Improvement Using Autonomous Soaring	Michael Allen	15
X-43C VSD Loading System	Mark W. Hodge	17
F-15 IFCS Neural Net	Dick Larson	19
Automatic Air Collision Avoidance System Initial Flight Test Evaluation	Mark Skoog	21
Orbital Space Plane	Chris Nagy	23
C-17 REFLCS	John Saltzman	24
NASA C-17 PHM Data Fusion Development	Matt Molzahn	26
Visualization Tools for Vibration Data	Philip J. Hamory	28
Updated Miniature 3-Axis-Vibration High-Frequency Data Logger	Philip J. Hamory	31
Relative Navigation Technique to Support the Development of a Refueling Drogue Model	Glenn Bever	33
Development of STARS Phase 2 Range User System Flight Hardware	Robert Sakahara	35
Flight Tests of Phase-1 Space-Based Telemetry and Range-Safety Study	Robert Sakahara	37
Flight Tests of Enhanced Flight Termination System (EFTS)	Robert Sakahara	39
Dryden Aerospike Rocket Test	Trong Bui	41
C-17 Propulsion Health Monitoring	Trindel Maine	43
Carbon Composite Control Surface Test Program	Larry Hudson	45
NGLT C/SiC Bodyflap Control Surface Test Program	Larry Hudson	47
X-37 Hot-Structure Control Surface Development Program	Larry Hudson	49
NASA Dryden "Virtual Flight Loads Lab"	Allen Parker	51
Fiber Optic Sensor Attachment Development and Performance Evaluations	Anthony Piazza	53
Data Decompositions and Nonlinear Identification for AAW Aeroservoelastic Data Analysis	Marty Brenner	55
48,000-Lb Capacity Aircraft Jack and Soft Support System (48K-3S)	Starr Ginn	57
Creating Detailed Structural Dynamic Finite Element Models Using PATRAN	Starr Ginn	59
14,240-Lb Capacity Overhead Soft Support System (3S)	Starr Ginn	61

<u>Title</u>	<u>First Author</u>	<u>Page</u>
HXRV3—Horizontal Tail Ground Vibration Test Results	Starr Ginn	63
Mode Matching Technique for the Finite Element X-Plane Pylon Models	Natalie Spivey	65
Equivalent Beam Modeling of X-43A Stack (Ship 2) Using Mode Matching Techniques	Natalie Spivey	68
X-Plane Pylon and B-52H Ground Vibration Test	Natalie Spivey	73
AAW Twist Model Development	Andrew Lizotte	76
DC-8/Lightweight Rain Radiometer Dynamic and Flutter Modeling	Chan-gi Pak	78
Generation of B-52H Mother Ship Dynamic and Flutter Models	Chan-gi Pak	80
X-43A Wing Control Horn Dynamic Modeling, Verification and Aeroelastic Effects	Roger Truax	83
Aeroservoelastic Stability Analysis of X-43A Stack	Chan-gi Pak	85
Flight Investigation of Prescribed Simultaneous Independent Surface Excitations (PreSISE) for Real-Time Parameter Identification	Tim Moes	87
Tech Briefs and Patents		89

2003 Research Engineering Directorate Staff

Director (Acting)
Deputy Director
Associate Director (Acting)
Administrative Officer

Patrick Stoliker
Vicki Regenie
Brad Flick
Everlyn Cruciani

Branch Codes and Chiefs

RA – Aerodynamics
RC – Controls and Dynamics
RF – Flight Systems
RI – Flight Instrumentation (Acting)
RP – Propulsion and Performance
RS – Aerostructures

Al Bowers
Joe Pahle
Bob Antoniewicz
Don Whiteman/Ting Tseng
Dave Lux
Steve Thornton

Automated Aerial Refueling Hitches a Ride On AFF

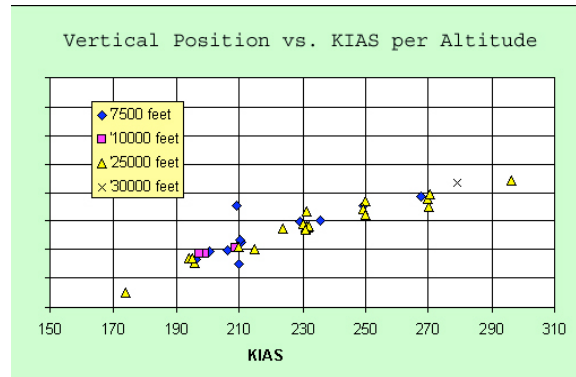
Current Need

The recent introduction of UAVs into the airspace has spawned a new era of autonomous technologies and challenges. Automated aerial refueling (AAR) is a capability that will enable UAVs to travel greater distances and loiter longer over time-critical targets. NASA Dryden Flight Research Center in cooperation with DARPA, NAVAIR, Naval Air Force Pacific Fleet, and the Air Force Research Laboratory conceived and successfully accomplished a fast response, flight research experiment focused on collecting a unique, high quality, database to validate hose and drogue dynamics. This flight-derived database would be used to validate modeled dynamics in support of automated aerial refueling system design and analysis for future UAV applications. The flight research was accomplished using two Dryden F/A-18 aircraft and an S-3 hose-drogue refueling store on loan from the Navy. The year-long project was started on Oct. 1, 2002, and completed 583 research maneuvers during 23 flights.



Approach

The team began with the full integration and instrumentation of the Aerial Refueling Store (ARS) with an F/A-18A aircraft, which had never previously been accomplished. After conducting envelope-expansion flights in Dec 2002 for NASA 847 to carry and operate the ARS, the team focused on outfitting NASA 847 and NASA 845 each with a pair of cameras to record the movement of the hose/drogue system. Building on heritage technologies developed for the Autonomous Formation Flight (AFF) program, the hose/drogue effects were investigated at altitudes between 7500 and 30000 feet, and airspeeds ranging from 195 to 300 KIAS. The effects of flight condition, hose weight, tanker weight, and receiver approach speed and direction on the hose/drogue response were explored in a build-up fashion. AAR also borrowed AFF's GPS-based relative positioning capability to guide the trail aircraft into the proper position behind the tanker aircraft. Post-flight processing of the on-board videos yielded position and velocity data of the hose/drogue system.



Results

The freestream position, drogue drag, and the effects of turbulence on the drogue were investigated. The freestream position change of the drogue with flight condition is depicted above. Similar to the research of AFF, AAR explored many avenues, including video tracking and calibration methods, and flight test and piloting techniques. The unique configuration of the airplanes enabled the first-ever in-flight measurement of the hose and drogue drag. Preliminary analysis of the video-derived data is complete.

Contacts

Jenn Hansen, DFRC, Code RA (661) 276-2052

Jim Murray, DFRC, Code RA (661) 276-2629

Real-Time Stability and Control Derivative Estimation with the F-15 #837 Aircraft

Summary

A real-time stability and control derivative estimation technique was used to support flight demonstration of an indirect-adaptive Intelligent Flight Control System (IFCS) concept. Traditionally, parameter identification (PID) is done post-flight. For the indirect-adaptive IFCS concept, however, in-flight PID is required so that the system can modify control laws for a damaged aircraft. The use of such a PID technique was demonstrated on a highly-modified F-15.



Objectives

The main objective was to estimate, in near real-time, the stability and control derivatives of the aircraft. A secondary goal was to develop a system to automatically assess the quality of the results, so as to tell a learning neural network what data to train on.

Approach

Parameter estimation was done using a technique called Fourier Transform Regression (FTR), which was developed at NASA Langley. FTR is an equation-error technique that operates in the frequency domain. Data are put into the frequency domain by using a recursive Fourier transform for a discrete frequency set. This simplifies many calculations, removes biases, and automatically filters out data beyond the chosen frequency range.

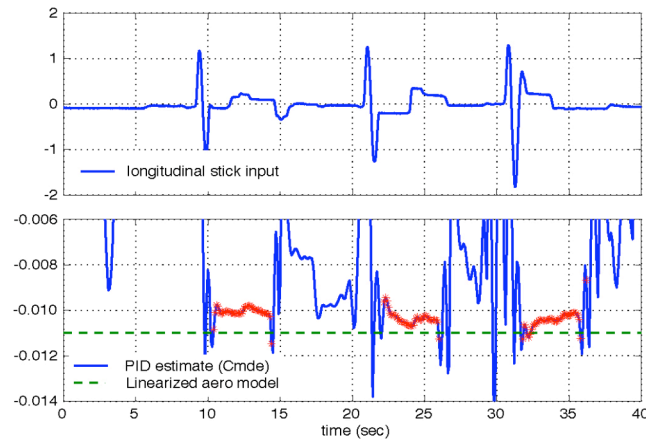
The FTR technique was tailored to work with pilot inputs, which produce correlated surface positions that prevent accurate parameter estimates, by replacing half the derivatives with predicted values. FTR was also set up to only work on a recent window of data, to accommodate changes in flight condition.

A system of confidence measures was developed to identify quality parameter estimates that a learning neural network could use. This system judged the estimates primarily on their estimated variances and on the level of aircraft response.

The resulting FTR system was implemented in Simulink and autocoded in C for use on the Airborne Research Test System (ARTS II) computer installed on the F-15. The Simulink model was also used in the control room using the Ring Buffered Network Bus (RBNB), making it possible to evaluate test points during flights.

Results

In-flight parameter estimation was done for piloted and automated maneuvers, primarily at three test conditions. The figure shows results for pitching moment due to symmetric stabilator for a series of three pitch doublets. A window of 5 seconds was used. Highlighted points are ones that passed the confidence tests.



The technique showed good convergence for most derivatives for both kinds of maneuvers, typically within a few seconds. The confidence tests were marginally successful and would need to be refined for IFCS use.

Contacts

Mark Smith, DFRC, RA (661) 276-3177

Tim Moes, DFRC, RA (661) 276-3054

Gene Morelli, LaRC (757) 864-4078

Development and Testing of a Drogue Parachute System for X-37 ALTV / B-52H Separation

Summary

One of NASA's primary responsibilities on the X-37 ALTV project is to ensure a safe, clean separation of the X-37 ALTV from the B-52H. If a post-drop re-contact between the X-37 ALTV and B-52H were to occur, there is a high potential for significant damage including the loss of one or both vehicles. Multiple scenarios were identified where the X-37 Approach and Landing Test Vehicle (ALTV) catastrophically re-contacts the B52H carrier aircraft after separation. (Figure 1)

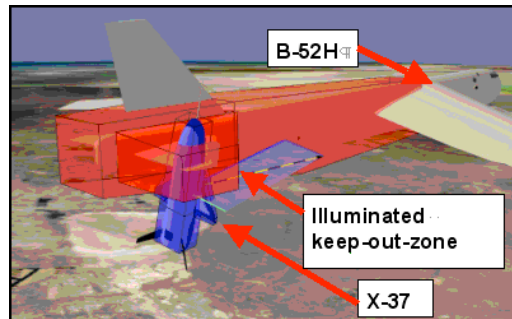


Figure 1: X-37 Re-contacting B-52H Tail Area

The most cost-effective re-contact risk mitigation is the pre-launch deployment of a drogue parachute that is released after the X-37 ALTV has safely cleared the B-52H. After release a fully inflated drogue chute takes 30 minutes to reach ground and results in a large footprint that excessively restricts the days available for flight. To reduce the footprint a passive collapse mechanism, consisting of an elastic reefing line attached to the parachute skirt, was developed. At flight loads, the elastic is stretched and allows full chute inflation. After release drag loads drop dramatically and the elastic line contracts to reduce the frontal drag area. A 50% drag reduction results in an approximately 75% reduction in the ground footprint. Eleven individual parachute designs were evaluated at flight-load dynamic pressures in the High Velocity Airflow System (HIVAS) at the Naval Air Warfare Center (NAWC). Various options for the elastic reefing system were also evaluated at HIVAS. Two best parachute designs were selected from HIVAS and will be carried forward to flight-test.

The design challenges for the X-37 ALTV drogue chute were significant. The program requirements for high speed, long duration deployments of a high-drag, small diameter, high stability parachutes broke new ground. Chute designs of this specific nature had never been constructed and tested. The unstable nature of the X-37 ALTV required that the chute properties be very accurately characterized. Small changes in the chute design features had dramatic effects on the overall performance and durability. The lessons learned from the three phases of HIVAS testing were well learned and a successful set of parachute designs that met all of the X-37 ALTV requirements emerged.



Figure 2: Candidate X-37 Drogue Chute Design During Test at HIVAS

Technical Contacts:

Tony Whitmore	DFRC RA (661) 276-2002
Steve Jacobson	DFRC RC (661) 276-7423
Steve Jensen	DFRC RS (661) 276-3841

Application of CONDUIT to the Active Aeroelastic Wing

Summary

The Active Aeroelastic Wing (AAW) program is investigating the characteristics of an aeroelastic wing and the technique of using wing twist for roll control. The design tool adopted by Dryden for the control law design is called CONDUIT (Control Designer's Unified Interface), which was developed by the Army/NASA Rotorcraft Division at the NASA Ames Research Center. It is a control system design tool that uses a multi-objective function optimization to tune selected control system design parameters.

Objective

The primary objective of the project is to demonstrate the use of wing twist on an aeroelastic wing to roll the aircraft. In doing so, the design will seek to maximize roll rate without the use of the rolling tail, while maintaining loads within their structural limits. Stability margins will be maintained, as will handling qualities criteria. The second objective will be to provide future aircraft designers with a tool, and design guidance, for the incorporation of AAW technology in future aircraft designs.

Justification

The Phase II control law flights will demonstrate the applicability of CONDUIT to the design of future AAW aircraft. Furthermore, they will demonstrate the characteristics and capabilities of an aeroelastic wing.

Approach

The Phase I derived aerodynamic increments and structural loads model were incorporated into the Dryden AAW simulation and CONDUIT respectively. A typical use of CONDUIT would normally employ a linear aircraft model within a Simulink block diagram for time history simulations. To provide for greater fidelity in the AAW design, the nonlinear AAW simulation was incorporated into CONDUIT for time history analysis. This integration required significant modifications to both the nonlinear simulation and CONDUIT. Frequency analysis was performed using a linear model in conjunction with a Simulink block diagram. The design parameters of the optimization consisted primarily of four gains, one for each wing surface, which defined their relative deflections. In CONDUIT, optimization constraints and objectives are defined as specifications. First and foremost, specifications were included to satisfy stability margins. Following those were the structural loads specifications, to ensure that wing root bending/torsion, wing fold bending/torsion, and wing surface hinge moment limits were constrained to within their design limits. Additional specifications were added to ensure adequate handling qualities. Time to bank and maximum roll rate specifications were created and used as objectives of the optimization. Two approaches were taken for the optimization. For lower dynamic pressure test points, where the aileron was effective and not reversed, CONDUIT was allowed to minimize time to bank by any means. For the higher dynamic pressures, where the aileron is ineffective at creating rolling moments but effective in producing wing torque, a wing twist methodology was used. That is, the leading edge flaps were deflected, twisting the wing, and the aileron was used to control wing root and fold torsion.

Status

The Dryden control law design effort has been completed. Of the eighteen flight conditions to be flown, nine will evaluate the Dryden designed gains. The remaining flight conditions will evaluate Boeing designed gains. Phase II flights will start in the Fall of 2004.

Contact

Ryan Dibley, DFRC, RC, (661) 276-5324

ryan.dibley@dfrc.nasa.gov



AAW Loads Model Verification and Validation

Background/Objectives

One goal of the Active Aeroelastic Wing (AAW) project is to demonstrate roll control using wing twist. This will be accomplished through flight tests of a new control law developed with the accurate loads models. Phase-1 flight tests using piloted and control surface double maneuvers were used to derive a loads model for the AAW aircraft. This model has now undergone extensive testing to ensure correct implementation into the simulation and to ensure its validity.

Verification Testing

The loads model was implemented into the AAW piloted 6-DOF simulation according to the controlled loads model description document. Check cases were run in both the simulation and in the Matlab scripts used to generate the model. Perfect comparison of the resulting loads verified the loads model implementation.

Validation Testing

Validation testing was conducted in a number of different ways. First, the output of the loads model for each flight condition and load was compared with flight data using the maneuvers used to create the model and with independent maneuvers that were reserved for testing only. The results of one of these tests are given in figure 1.

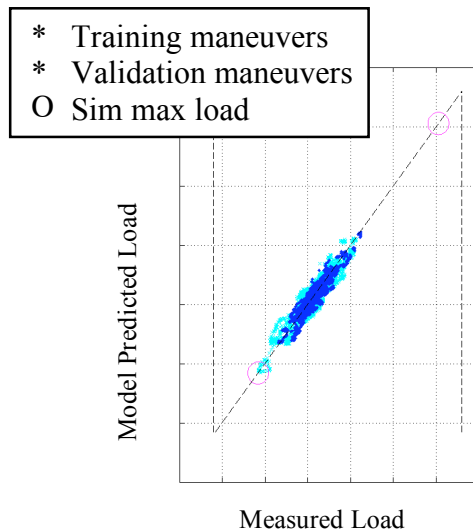


Figure 1. Wing root torque load validation.

Figure 1 shows the measured and predicted load for all maneuvers flown at that flight condition. A circle representing the expected load during phase-2 flight is also included to show the loads model extrapolation from phase-1 data.

Further validation testing was accomplished by comparing the model predicted loads during surface doublet maneuvers flown in the simulation to surface doublet maneuvers flown in phase-1 flights. A time history from one of these tests is given in figure 2.

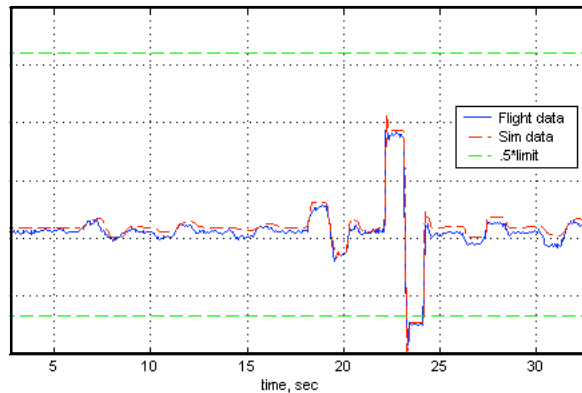


Figure 2. Comparison of simulated load to flight data.

The simulation tests validated the simulation of loads on the AAW aircraft and demonstrated the accuracy of the aerodynamics and loads models working together.

The individual terms of the loads model were also plotted versus dynamic pressure and checked for continuity. These checks showed a reasonable progression with dynamic pressure with a large jump from subsonic to supersonic flight conditions.

Most recently, loads model testing at neighboring flight conditions was performed to check the sensitivity of the model to variance in Mach and altitude. Results from this work showed good model predictability except at Mach = 0.95 where a known nonlinearity exists on the aileron and trailing edge flap hinge moments with Mach number.

Documentation

The derivation steps, units, scaling, and calculations used to create the loads model are given in: *AAW_NASA_Loads_Model_Description1_8.doc*. This document is under project CCB control. The verification and validation test description and results are given in: *AAW_NASA_Loads_Model_VnV2_0.doc*. A NASA TP with loads model derivation, testing, and final results will be published after completion of phase-2 flight test.

Conclusion

Loads model verification and validation testing has demonstrated the successful implementation of an accurate loads model into the AAW simulation.

Point of Contact

Michael Allen
NASA Dryden Flight Research Center
(661) 276-2784

Vortex-Induced Navigation Experiment (VINE)

Summary

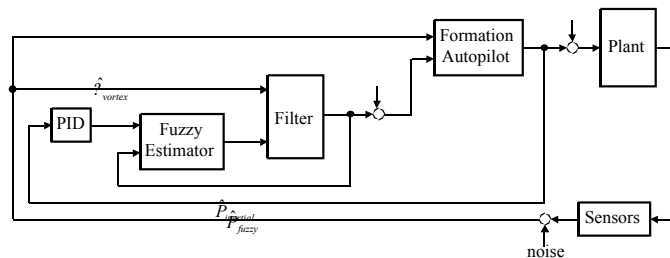
The Vortex-Induced Navigation Experiment (VINE) is studying a method for estimating the relative position between two aircraft in close formation flight through real-time estimates of the aerodynamic effects imparted by the leading airplane's wingtip vortex on the trailing airplane. A fuzzy algorithm to map combinations of vortex-induced drag and roll effects to relative position was developed and integrated with a leader-follower formation flight autopilot in a two-ship F/A-18 simulation. Good closed-loop control was achieved in the lateral-axis and significant progress has been made toward achieving a two-axis solution.

Objective

The goal of VINE is to alleviate pilot workload during precision formation flight without the use of inter-aircraft communications. Recent flight tests at Dryden have shown that fuel savings of 10% or more can be achieved by flying two F/A-18s in close formation. The high workload experienced by the pilot during these tests demonstrates the need for a formation autopilot in any realistic commercial application. However, the relative navigation and communication systems needed to support automated formation flight can be expensive and logistically limiting. VINE will identify whether knowledge of an aircraft's trim state within a wingtip vortex is sufficient to estimate its location relative to the leading aircraft; and, if so, determine the usefulness of that estimate as a feedback signal to a formation autopilot.

Approach

The VINE system consists of a formation autopilot, a parameter identification (PID) routine, a fuzzy estimator and a complementary filter. The formation autopilot controls the lateral and vertical relative positions between the aircraft. The PID routine estimates the vortex roll and drag effects from the autopilot trim commands. These are used by a fuzzy logic algorithm to estimate the current relative position. The low frequency portion of this estimate is combined with the high-frequency portion of a second relative position estimate based on the local aircraft's state feedbacks.

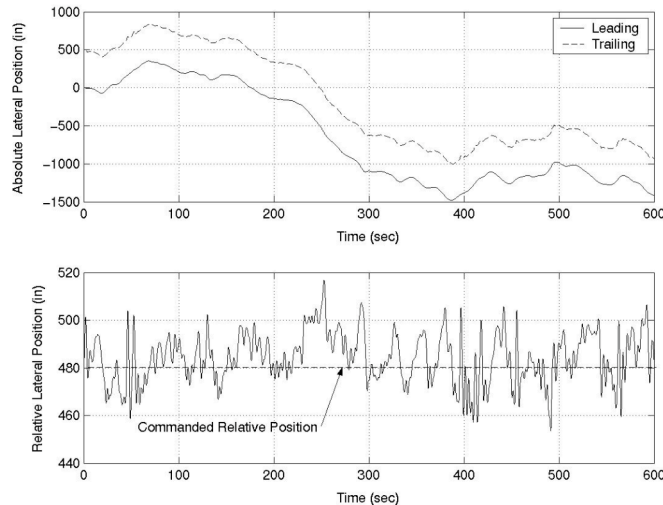


VINE Block Diagram.

Because this is a workload-alleviation system rather than a fully autonomous controller, the pilot is responsible for initially stabilizing the aircraft within the wingtip vortex. Once VINE has begun to provide valid relative position estimates, roll and pitch control can be turned over to the formation autopilot. A low-level of pilot throttle input is then required, in conjunction with a velocity-hold autopilot, to modulate longitudinal spacing.

Results

A lateral axis VINE system for two F/A-18 aircraft has been designed using a theoretical vortex model and tested in simulation. In conjunction with an altitude-hold autopilot, the VINE system was generally able to track lateral motions of the leading aircraft to within about ± 24 inches. This is well within the ± 72 inch accuracy requirement to achieve a sustained drag reduction of at least 10%. Additional work has been done to expand the fuzzy estimator to both the lateral and vertical axes using data from the Autonomous Formation Flight (AFF) Phase 1 Risk Reduction flight tests. Static estimates accurate to approximately ± 24 inches have been obtained in both axes.



Single-Axis VINE Simulation Results

Status/Future Work

The fuzzy algorithm must be refined to achieve stable, closed-loop control simultaneously in the lateral and vertical axes. Algorithm sensitivity to such things as uncertainty in the design models, errors in the PID estimates and dynamic changes in the vortex size, strength and location will be studied.

Contact

Curtis E. Hanson, Principal Investigator
NASA Dryden, Code RC x3966

Evaluation of Optimal Control Allocation Methods for C-17 IFCS

Summary

Several control allocation (CA) schemes were evaluated for use in the C-17 IFCS 2nd generation control laws. The challenge for CA is to optimally distribute control effect, through control surface deflections, when presented with position or rate limited control surfaces. Both optimal and sub-optimal methods were evaluated emphasizing computational performance and solution accuracy. Optimal CA methods can be divided into two general classifications based upon the form of their cost function. Error minimization methods attempt to minimize the difference between the achieved and the desired control objective. Direction preserving CA methods attempt to minimize error while maintaining the direction of the desired control objective.

Objective

The study's purpose was to evaluate the accuracy, computational time, and aircraft response of the C-17 IFCS 2nd generation control laws with several optimal and sub-optimal control allocation methods. The goal of the evaluation was to determine the suitability of each CA method for continued research.

Approach

Testing of the CA methods was performed with a linear C-17 model in Simulink. A non-adaptive, simplified dynamic inverse controller, with P+I control, provided control commands to drive the CA methods. Actuator failures were included to test the ability of the CA methods to redistributed control authority and to impose a condition in which several of the healthy actuators were driven to their physical limits. The error, magnitude and angle, of the CA solutions were evaluated at each frame of the simulation. Computational time was also evaluated. The selection of suitable methods for further evaluation was a trade-off between accuracy to a known optimal solution and computational intensity.

Results

Several CA methods have been found to be suitable for implementation with the C-17 IFCS 2nd generation control laws. Time histories for two CA methods are shown in Figure 1 and Figure 2. Figure 1 shows the ability of the two methods to track the commanded roll, pitch, and yaw doublets in the presence of multiple actuator failures. The error and surface usage of the two methods is shown in Figure 2. In general, the "moqp" method is able to track the command more accurately than the "daisy" method. The cost of this improved tracking is computation time; "moqp" requires 6x the computational time of the "daisy" method.

Status

Further work is being conducted to incorporate the CA methods into a portable library to allow rapid evaluation in non-linear simulations.

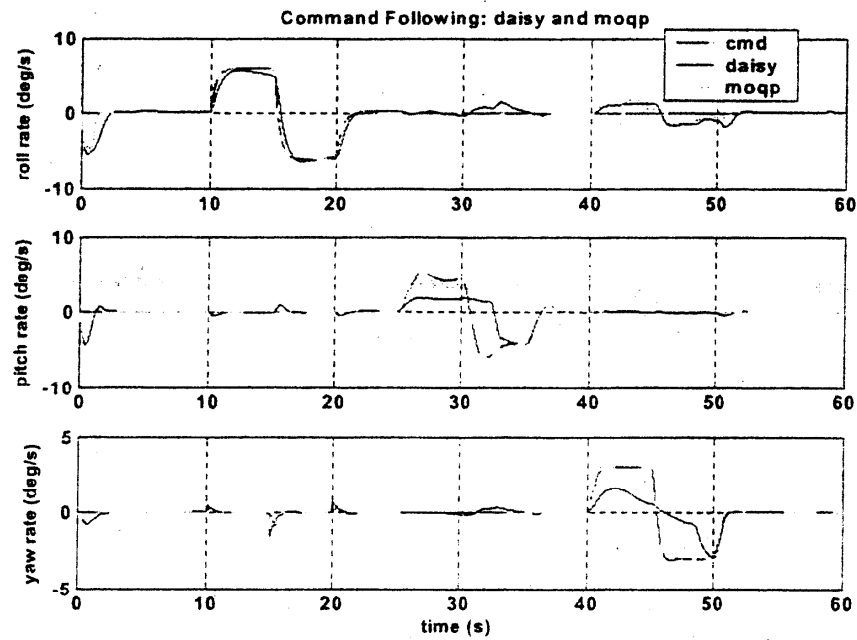


Figure 1. Command tracking of two control allocation methods.

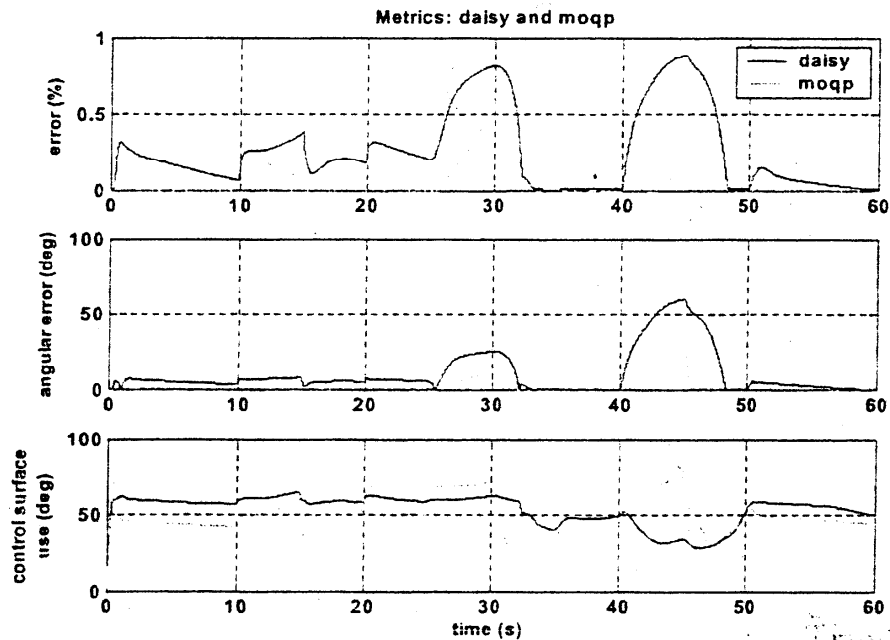


Figure 2. Error and control surface usage of two control allocation methods.

Contact

Chris Regan, NASA Dryden, RC, x5696

UAV Endurance Improvement Using Autonomous Soaring

Background/Objectives

A relatively unexplored way to improve the endurance of an autonomous aircraft is to use buoyant plumes of air found in the lower atmosphere called thermals or updrafts. Updrafts are commonly used by glider pilots and birds to improve range, endurance, or cross-country speed. A quantitative analysis of a small electric-powered UAV using thermal updrafts to extend its endurance over a target location was performed to determine the potential benefit of autonomous soaring. A 3-degree-of-freedom simulation of the UAV was used to determine the yearly effect of updrafts on performance.

Updraft Model

An analytical updraft model was developed for this effort using surface weather measurements and updraft equations from NCAR flight data. Surface radiation and rawinsonde balloon measurements taken at Desert Rock, NV were used to determine convective-layer scale factors that were then used to determine the size, strength, spacing, shape, and maximum height of the updrafts for the simulation. Updraft positions were randomly chosen and were given a lifespan of 20 minutes.

Simulation

UAV simulation was accomplished with a 3 degree-of-freedom, Matlab-based simulator. The simulation was run with updraft data from each day of the year 2002 to determine yearly trends in soaring performance. During each run, the UAV searched for updrafts by flying a spiral ground track until an updraft was encountered. An encountered updraft was utilized by circling within the updraft. The simulation assumes that an autopilot and soaring algorithms exist to sense and utilize an updraft after it has been encountered by the UAV. Simple updraft detection and utilization algorithms have been designed and simulated by other researchers.

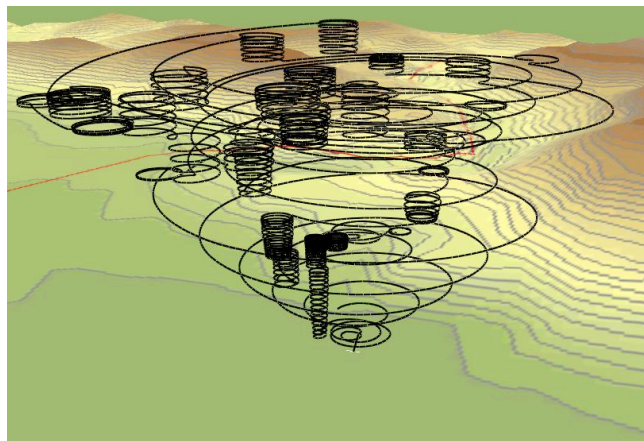


Figure 1. Typical UAV path during loiter mission. Line of sight to the ground target is always maintained.

Results

Results show that a UAV with a nominal endurance of 2 hours can fly up to 14 hours using thermal updrafts during the summer and up to 8 hours during the winter. Seasonal variations are due to changes

in length of day and sun angle. The performance benefit and the chance of finding updrafts both depend on what time of day the UAV is launched. Late morning launches were found to give the best overall performance and chance of success. Yearly average endurance was found to be 8.6hr with these launch times. Sensitivity studies show low sensitivity to aircraft performance, as well as updraft lifespan, height, and spacing. Broad applicability of this technology is expected because of the wide range of insects, birds, and manned gliders that soar world-wide.

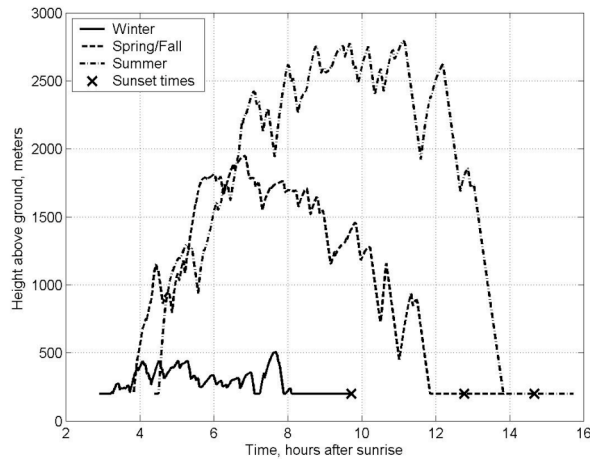


Figure 2. Typical altitude time histories showing seasonal variations.

Documentation

This work is a result of a FY03 DDF and has resulted in a paper titled “Autonomous Soaring for Improved Endurance of a Small UAV” to be presented at the AIAA conference in Reno NV, January 2005.

Conclusion

An analytical updraft model was developed using measured meteorological data and updraft equations derived from flight data. The updraft model was integrated into a simple UAV simulation to determine yearly endurance gains. Results show that significant endurance improvement can be obtained year-round using convective lift for a small UAV.

Point of Contact

Michael Allen
Michael.J.Allen@nasa.gov
(661) 276-2784

X-43C VSD Loading System

Summary

The Next Generation Launch Technology office at Marshall Space Flight Center has introduced a program as part of the Hyper-X flight program activity called X-43C. NASA Langley as project office and NASA Dryden as the flight test facility, including the USAF, are developing three hypersonic flight vehicles designated as X-43C. The X-43C free flyer, called the demonstrator vehicle shall demonstrate the performance of an air breathing, scramjet engine burning hydrocarbon fuel in a hypersonic flight environment. The demonstrator vehicle (DV) is to demonstrate sustained acceleration from Mach 5 to Mach 7. The DV is to be dropped from a carrier aircraft and boosted to its predetermined test condition by a modified Pegasus rocket first stage. The DV will separate from the rocket stage and start its scramjet engine and accelerate for a predetermined time. The vehicle will then conduct specified maneuvers and drop in the ocean.

Before the DV is flown it must pass validation testing. NASA Dryden is developing a ground test platform to prepare the DV for validation testing. This platform and associated systems is called the vehicle systems demonstrator (VSD). A wing surface loading system has been developed to perform compliance and fin root bending testing. The system is also for applying surface loads during simulation runs to provide a resemblance of reality.

Approach

A self contained portable system designed to accurately apply loads to the X-43C VSD moving surfaces was designed by Dynamics Controls Incorporated in Dayton Ohio. The system provides both loading and data collection. The system provides large surface movements with minimal effect on the applied loads.

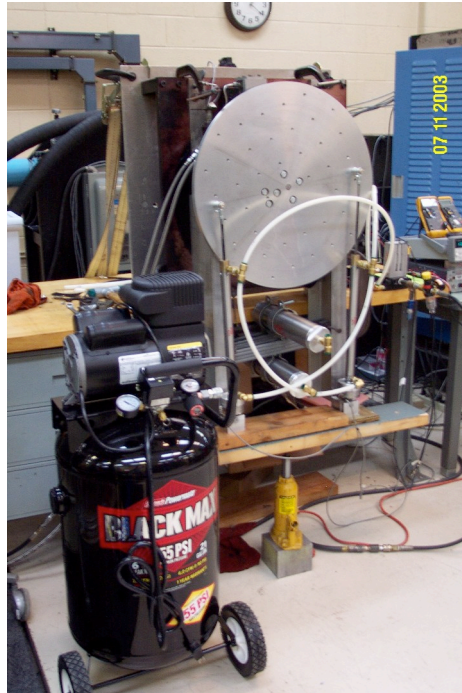
The system uses two separate units, a power unit and an electronic unit. The two units are connected by electronic cables for control.

The power unit has 4 pneumatic servovalves mounted on a manifold with gauges and shut-off valves. The unit operates near the VSD using nylon tubing to deliver air pressure to pneumatic load cylinders.

The load cylinders with precision load cells will be attached to the moving surfaces and a mechanically ground reaction frame. The load cylinders have custom made low friction bearings to minimize cylinder resistance to load changes. The load cylinders have a stroke of 12 inches and a force capability of nominally 100 pounds. A National Instruments LabView system provides the data collection capability for the electronics unit.

Results

Below is a preliminary test set up of the system using a hydraulic positioning table. The system is to be delivered to Dryden in March of 2004.



Contacts

VSD Lead:

Mark W. Hodge DFRC, RF, (661) 276-7528

F-15 IFCS Neural Net

Summary

The F15 837 airplane underwent hardware and software modifications in support of GEN I flights. An Analog Multiplexer AMUX box was interfaced to allow parameters to be input to the ARTS II computer, which was used for real time PID estimations in support of GEN I. These signals were calibrated and scaled during ground validation testing on the airplane. Also, 1553 bus broadcast messages were added to the ARTS II for telemetering and recording on the NASA instrumentation system. The new ARTS II software also included the saving and time logging of pertinent signals in nonvolatile random access memory (NVRAM) in the ARTS II processor that was used for post flight data retrieval.

The GEN I flight phase ended after completing 11 flights by the summer of 2003. The Real-time Parameter Identification (PID) estimate algorithms were successfully validated during this phase. The neural net for this phase featured an online learning design called Dynamic Cell Structure (DCS). This design learns the changes in the stability and control derivatives identified by the PID algorithm.



The GEN II phase was started which incorporates a new neural net (NN) design called Sigma Pi. This system is designed to be flight-tested using simulated actuator failures. The intent is to evaluate the NN's ability to reconfigure surface control connections so that a level 1 flying quality aircraft is maintained.

Objectives

The GEN I program objectives were to use a NN to identify aircraft stability and control properties for use in optimizing aircraft performance. The GEN II objectives are to use a more general NN design to optimize control of the airplane for nominal and simulated surface failures.

Approach

Host the Sigma Pi Neural Net software Operational Flight Program (OFP) on the flight experimental computer called Airborne Research Test System (ARTS II). Engage this controller in a closed loop mode on the airplane. Since this is a single channel controller, develop safety monitors to protect the airplane against errant commands, which may cause structural damage or unacceptable transients to the airplane. Develop system requirements to meet safety and mission success criteria. Evaluate and test

the software using a closed loop, piloted simulation at DFRC and the hardware in the loop simulation (HILS) at Boeing Phantom Works.

Install the new OFP's for both the Flight Computers (FC) and the flight unit ARTS II computer. Develop procedures to perform functional testing on the aircraft including Structural Mode Interaction (SMI) to validate the notch filters.

Part of the safety monitor concept is a loads monitor, which will be hosted on the SCE-3 part of the FC. This monitor will be validated by flight test. The airplane has been instrumented with strain gages to record loads data, which will be crosschecked with the loads monitor.

Modification to the pilot vehicle interface (PVI) has been designed to allow Sigma Pi engagements and failure insertion. This design will be evaluated with piloted simulations to confirm functionality. Also perform failure modes evaluation to confirm fault detection, research experiment disengagement, safety monitor operation, and transient characteristics.

Results

The GEN I phase was successfully completed. The Sigma Pi NN design for GEN II is nearing completion.

Status

The Sigma Pi and the Versatile Control Augmentation System (VCAS) design is nearing completion. Safety monitor concepts will be tested for fault detection, transient suppression, and structural load protection using the DFRC simulation. The loads monitor is currently in the process of being integrated in the flight hardware at BPW. Once the Sigma Pi and VCAS software is baselined, then integration, verification, and validation testing will be performed. The goal is to flight test this system later this year.

Contact

Dick Larson, IFCS Flight Systems Engineer
NASA DFRC, RF, (661) 276-3740

Automatic Air Collision Avoidance System Initial Flight Test Evaluation

Summary

The Automatic Air Collision Avoidance System (Auto ACAS) program was a joint USAF and Sweden effort addressing the see and avoid challenge of aviation. The Auto ACAS was a modular architecture intended to easily be adapted to any aircraft architecture, platform and mission. The architecture was centered in a software executive that fused sensor information to a collision prediction algorithm. If proximity criteria were met within the collision prediction, the aircraft operator was alerted. An automatic evasion maneuver would be executed if the collision potential continued to worsen and the automatic evasion option was selected. The system executed internal monitoring for integrity to aid in safety of operation. The aircraft employed for Auto ACAS testing was an F-16C airframe with Block 50 avionics, an F-16D airframe with Block 50 avionics, and the Variable Stability In-Flight Simulator Test Aircraft (VISTA). The Auto ACAS was jointly developed by SAAB Aircraft Linköping, Boeing Aircraft Company St. Louis, Missouri, Lockheed Martin Aeronautics (LM Aero), Fort Worth, Texas, Bihle Applied Research, Hampton, Virginia, Veridian Engineering in Dayton, Ohio, and Veridian of Buffalo New York. Flight test was conducted out of the USAF Test Pilot School under the technical direction of NASA DFRS. Forty flights over 29 missions totaling 68.9 flight hours were executed. Flight test locations included Edwards AFB in California, Fort Worth Texas and Eglin AFB in Florida.



Objective

The overall test objective was to evaluate the Auto ACAS ability to prevent mid-air collisions while at the same time not interfere with the normal operations of a fighter aircraft. This resulted in a need to determine the minimum amount of time required to avoid a collision by an algorithm-sensor suite. Previous testing of an automatic ground collision avoidance system had shown that maintaining large buffers between the aircraft and other obstacles could easily provide collision avoidance. However, these buffers would regularly require avoidance maneuvers that pilots deemed unwarranted and an impedance to normal mission operations. Concern existed that requirements for UAV see and avoid sensors might be generated that would require larger detection ranges or shorter detection times, thus driving up system cost.

Approach

To address the test objectives, collision geometries were required that went beyond what could be allowed for safe flight test conduct. Extremely hazardous collision geometries were conducted in flight against virtual aircraft. Avoidance performance using virtual aircraft was then validated under less hazardous collision geometries with actual 2-ship runs.

Many options existed within the Auto ACAS to investigate potential aircraft integration options. The Auto ACAS monitored neighboring aircraft state through either cooperative or non-cooperative sensors. The cooperative sensor used for these tests was a standard USAF data link. The data link shared position, intended escape path, and critical health information to other aircraft on the data link network. The non-cooperative sensor used for these tests was the APG-68 radar of the F-16. The Auto ACAS algorithm computed an optimum escape trajectory based on predicted future flight paths. The option existed for one, some or all aircraft to execute avoidance maneuvers. If more than one aircraft were executing avoidance maneuvers, their evasion directs were coordinated across the data link. Vehicle performance and health were critical factors in determining escape trajectory and the timing of initiating the avoidance maneuver. Multiple implementations of the Auto ACAS were tested. The VISTA aircraft utilized a consolidated architecture with avoidance algorithm and flight control co-located in the same processor. The F-16 utilized a federated architecture with algorithm and flight control processing distributed between multiple processors. Additionally, a virtual aircraft was implemented through the use of ground-based simulation. All architectures operated asynchronously with dissimilar frame rates.

Collision Avoidance Results

Preliminary results indicate that the Auto-ACAS was a robust system to prevent mid-air collisions. As tested, the Auto-ACAS supported a wide variety of potential integration approaches onto specific platforms. Simulation and virtual target testing correlated exceptionally well with flight test results, allowing the evaluation of this system under circumstances far too hazardous to test with real aircraft.

Flight test successfully accomplished 189 collision avoidance runs. Flight conditions ranged from 249 to 408 knots calibrated airspeed at altitudes ranging from 15,400 to 23,800 feet and aircraft gross weights from 22,800 to 31,400 pounds. Collision geometries at avoidance initiation ranged from co-heading to head-on, flight path angles 3 degree dive to 24 degree climb, normal load factors from 0.5 to 5.63 g, roll rates up to 45 degrees per second, airspeed differences up to 221 feet per second and closure rates from 101 to 1,767 feet per second. These runs included 2 or three aircraft on collision courses and consisted of a mix of piloted and UAV aircraft. In simulation, 467 successful runs were collected over a much wider range of conditions with up to 4 aircraft on collision course.

Integration errors in the Auto-ACAS flight test implementation resulted in some initiations of avoidance maneuvers too late to be certain of preventing collisions, however, these integration errors were identified and fixed following flight test. Evaluation of the fixed system in simulation showed mid-air collisions could consistently and reliably be avoided. The Auto-ACAS demonstrated exceptional ability to consistently prevent mid-air collisions under complex conditions. These conditions included cascading failures of critical components just prior to and during avoidance maneuvers with multiple aircraft in close proximity on collision courses. An Auto ACAS should be strongly considered for implementation onto any aircraft where a reduction in mid-air mishap rates is desired.

Contact:

Mark Skoog, DFRC RF, (661) 276-5774

Orbital Space Plane

Code R engineers supported the Orbital Space Plane (OSP) project office by assuming a primary role for the definition of Flight Test Services and Flight Test Facilities. This included the development of these sections for the Mod2 (contract extension) statement of work, work breakdown structure (WBS), and WBS Dictionary. Similar work was also accomplished for the project request for proposal. Unfortunately, neither of these two contracts were let because of the redirection of the project based on President Bush's space exploration initiative.

Code R engineers also developed a comprehensive set of flight test objectives to provide guidance to the contractors regarding what their test programs should demonstrate. These objectives were then used to evaluate contractor test plans. The "Flight Tests / Demonstrations" section of the OSP System Verification Plan was largely based on these objectives. A draft white paper was written outlining considerations for the flight test of an OSP vehicle.

During the year Code R engineers learned about the design proposals of each of the three (later reduced to two) contractors to better assess how they might be flight tested. This assisted the project in evaluating the test proposals presented at the System Operational Evaluation and the System Design Review. Scheduling constraints and the availability of test resources for both developmental and orbital flight testing were also evaluated.

Contact

Chris Nagy, NASA DFRC RF, (661) 276-2626

C-17 REFLCS

Objective

The intent of the C-17 REsearch FLight Computing System (REFLCS) is to demonstrate Intelligent Flight Systems (IFS) technologies in a real flight environment. One application of IFS technology to be demonstrated in flight is neural-net based Intelligent Flight Control System (IFCS) software. In a simulation environment, IFCS software has already demonstrated the ability to automatically compensate for degraded vehicle characteristics that may result from damage, control surface failures, or mis-predicted aerodynamics. The benefits range from the ability to land an airliner with failed hydraulic systems to return of a battle-damaged combat aircraft to increased robustness for a re-entry vehicle. Additionally, IFCS is a prerequisite for NASA's futuristic "morphing aircraft." Another application of IFS technology to be flight tested is an Integrated Vehicle Health Management (IVHM) system which will enable vehicle maintenance to be "need" based as opposed to "schedule" based. Also, the enhanced IVHM fault detection and reporting capabilities can be used to provide the capability to host IVHM elements within the IFCS flight controllers.

Approach

The REFLCS will be composed of a quad redundant set of Research Flight Control Computers (RFCCs) as shown in figure 1.

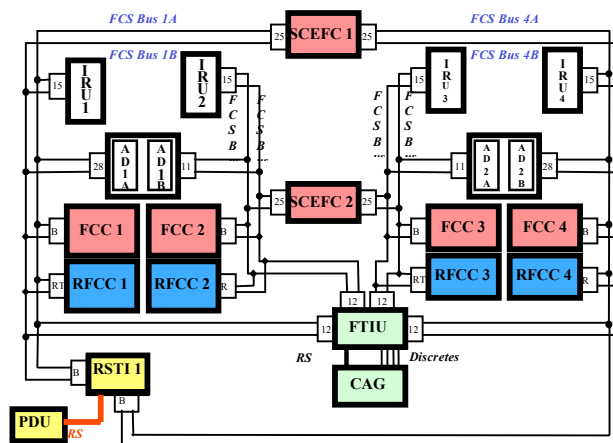


Figure 1. C-17 REFLCS Avionics Architecture.

In order to achieve the full complement of IFS objectives, the capability of the C-17 REFLCS will be enhanced through incremental builds.

Build 1 of the REFLCS will consist of replication C-17 control laws (CLAWS) in order to demonstrate that the REFLCS “tool-set” will function in a safe and effective manner to flighttest IFS technologies. Build 1 will function only in a limited (up and away) Class B envelope. Build 2 of the REFLCS will house Gen. 2.0 IFCS CLAWS (see figure 2 below) also in a Class B envelope with “simulated” fault insertion capability. Build 3 of the RELFCS is intended to be a full envelope (CLASS A) qualified system and will incorporate engine control and initial IVHM fault monitoring and detection.

Build 1 REFLCS is being developed by Boeing Long Beach with NASA Dryden oversight whereas, the NASA-Dryden Flight Systems branch is developing a REFLCS System Interface, which will provide

annunciation feedback to the pilots for Build 1. The Build 1 RSI consists of a REFLCS System Test Interface Computer (RSTI) and a Pilot Display Unit (PDU) referenced in figure 1. For Build 2, the RSI will be expanded to include a test interface to simulated failed control surfaces and change Gen 2 CLAW attributes. The Build 1 version of the RSI is currently being integrated and will be completed by the end of FY 2004.

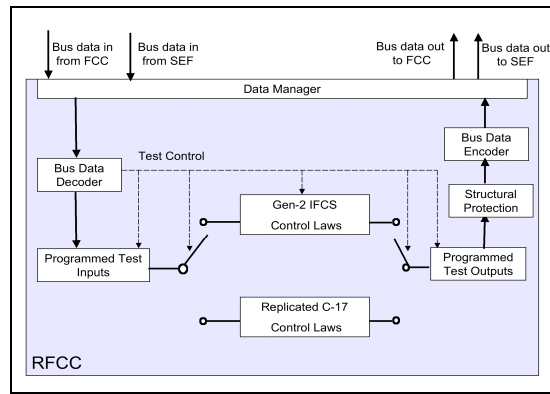


Figure 2. Build 2 RFCC Software Architecture.

Status & Future Work

Currently the project is focused on the development of REFLCS Build 1. Over the past year, the project has focused its efforts on mitigating risks with respect to structural protection. Build 1 subsystem and system level integration and test is currently set for end of FY 2004. Flight test of REFLCS Build 1 is currently scheduled to begin near mid FY 2005. Also, the Build 2.0 REFLCS System Requirements Specification (SRS) is currently being drafted to support Gen. 2.0 CLAW flight research. Concurrently, an effort is under way to build up an in-house Hardware-In-the-Loop-Simulation (HILS) of the C-17 REFLCS. The C-17 REFLCS HILS will support development, integration and test of future REFLCS builds to support IFS.

Contacts

John Saltzman, C-17 RF Lead (661) 276-3730

Curtis Hanson, C-17 RC Lead (661) 276-3966

Chris Cotting, C-17 Chief Engineer (661) 276-3797

NASA C-17 PHM Data Fusion Development

Summary

Recent dedicated NASA C-17 Propulsion Health Monitor (PHM) research flights have validated the airborne data fusion concept on heavily instrumented C-17 heavy lift class of vehicles. The demonstration also evidenced that a network centric and all COTS open computing solution is a viable approach to enhancing test and evaluation including both DOD (Air Force) and non-DOD (NASA) flight test community.

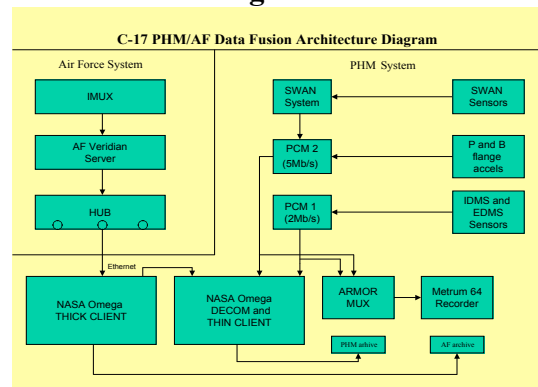
Objective

In support of NASA C-17 Intelligent Vehicle System (IVS) program, the NASA Dryden Research Instrumentation System Branch (RI) developed an airborne PHM instrumentation data system (PHM-IDS) for real-time quick-look visualization and validation of engine sensor and the ability to time correlate engine sensor measurements with C-17 T-1 highly instrumented vehicle avionic states (References 1 and 2). The ability to visually correlate in time multiple independently bussed sensor sources and vehicle avionic states is called data fusion.

Approach

The NASA PHM-IDS, an Omega-Serv based telemetry processing system (Reference 3), was required to be networked with the C-17 T-1 airborne Omega/IMUX system through a network hub. The architecture for this data fusion development is illustrated in figure 1. The architecture additionally required NASA to provide a dedicated client station serving as (1) an Omega Thick Client (from Omega/IMUX) and (2) as peer-to-peer server (to PHM-IDS). Finally, the data fusion visualization required an Omega Thin Client process on the PHM-IDS processing platform.

Figure 1.



Results

Typical data fusion results based on this airborne architecture have allowed the display and archive of time correlated engine sensor measurements with vehicle avionic states. These results provided the ability to acquire over 11,000 additional parameters to visualize the effects of the vehicle avionic states on the engine with minimum additional hardware.

Status

The NASA C-17 PHM research is still ongoing on the Air Force C-17 T-1 testbed and soon to be followed by the Research Flight Control System (REFLCS) and IVS. With anticipated future hardware

enhancements, data fusion with NASA PHM-IDS system can be extended to support REFLCS / IVS for any long duration mission. On the horizon, is the enterprise enhancements to the Omega-Serv, called the Omega Publisher (Reference 4), which the Omega Data Environment (ODE) will provide data publishing and data-on-demand universal data access, mining and distribution capability in support of PHM / REFLCS / IVS.

Contact

Matt Molzahn (Matt.Molzahn@dfrc.nasa.gov)

Mike Venti (Mike.Venti@dfrc.nasa.gov)

Tony Branco (Tony.Branco@dfrc.nasa.gov)

Glenn Sakamoto (Glenn.Sakamoto@dfrc.nasa.gov)

References

1. "C-17 AVIS No: PHM-DRD-001.01" dated February 10, 2003 by Mike Venti & John Orme.
2. "Interface Control Document for C-17 T-1 Engine #3 NASA Sensors & Instrumentation Rack C17-0000010", dated 6-16-02.
3. General Dynamics Advanced Information System (GD-AIS) - Omega MiddleWareToolset.
4. Data, Starving for Knowledge – Omega Data Environment", delivered at ITC October 2003, Las Vegas, Nevada.

Visualization Tools for Vibration Data

Summary

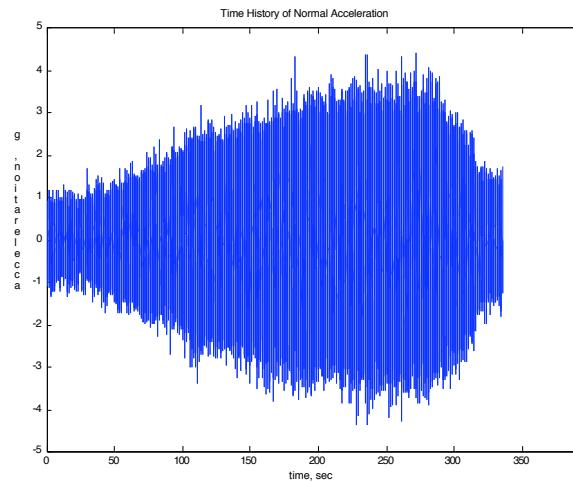
New tools for visualizing vibration data are in development.

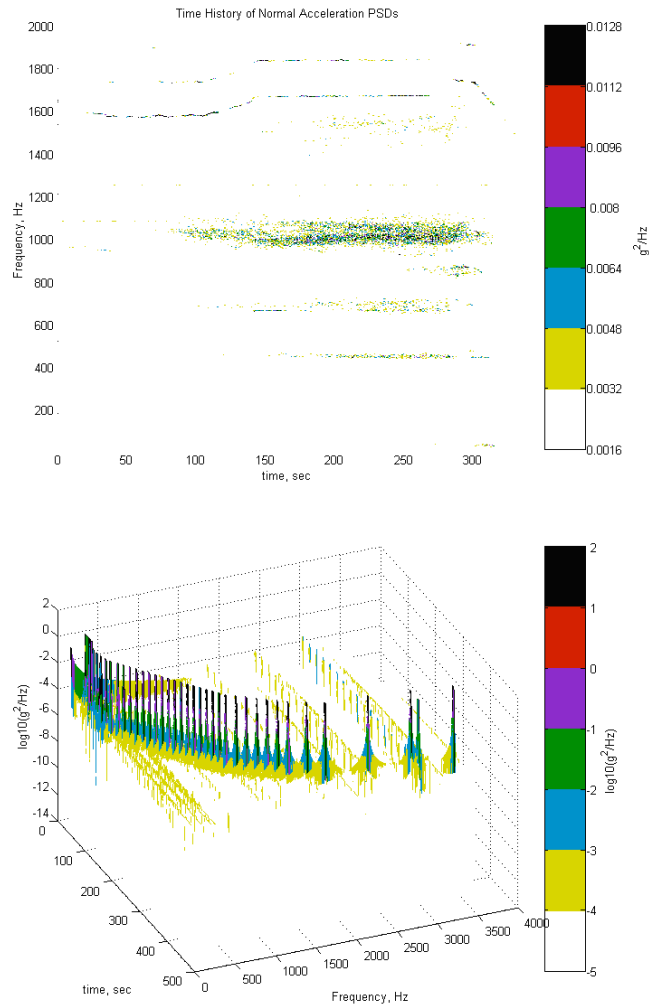
Justification

Sometimes both the time history and frequency content of vibration data are important. When high frequency data is collected over a long period of time, the volume of the dataset can make getting a quick overview of its content cumbersome. Tools for visualizing both the time and frequency content simultaneously are required and must be able to handle large files. When three-component vibration data is available, net directional results can be computed.

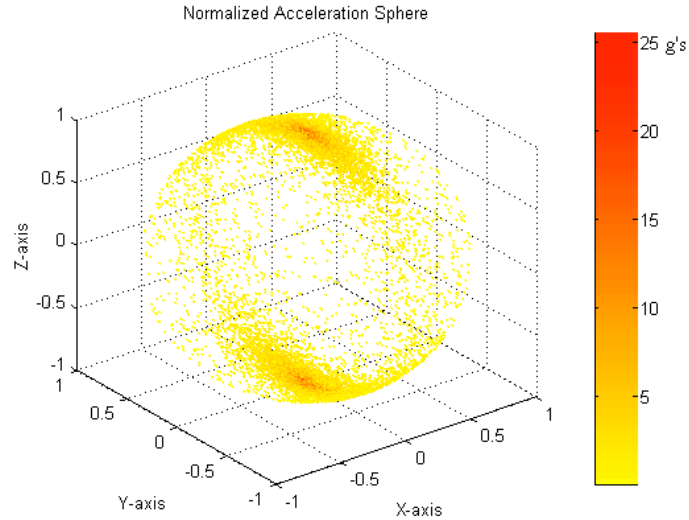
Approach

The approach is to build upon the capability that MATLAB (The MathWorks; Natick, MA) has for computations and plotting. One way to visualize the progression of power spectral densities (PSDs) over time is to plot time in one axis, frequency in another, and use color to represent the magnitude of the PSD. In the following example, normal-axis vibration data for an equipment bay of F-15B/836 during a slow level acceleration from Mach 0.95 to 1.85 and quick deceleration back to 0.95 is shown in two figures. The first figure is the time history and shows the increase and decrease of vibration over time. The second figure is the same data transformed to the frequency domain and plotted on the same time scale. In that figure the growth and decay of particular frequency components can be seen.





In a second example, the figure above shows the progression of PSDs over time for an accelerometer frequency response calibration. The time history would just show a constant magnitude of $\pm 10g$, but here peaks can be seen as the accelerometer is shaken at discrete frequencies over the seven-minute calibration.



In certain cases it is informative to visualize the magnitude and direction of accelerations experienced on a test article. The last figure is a 3-dimensional spatial representation of a vibration test conducted in the z-axis per curve A of Process Specification 21-2. The root-sum-square magnitude of the 3-dimensional acceleration is measured in g's and is represented by a color scale in which red (black in gray scale) indicates larger accelerations. The vector from (0,0,0) to each point is calculated and the magnitude is scaled to 1. This scaling situates all points on the surface of a unit sphere. Since this test was conducted on the z-axis, the red areas are centered about the top ($X = 0$, $Y = 0$, and $Z = +1$) and the bottom ($X = 0$, $Y = 0$, and $Z = -1$) of the sphere. A completely random vibration would appear as a sphere with points evenly colored and distributed along its surface.

Contact

Philip.J.Hamory@nasa.gov, (661)276-3090; Russell.J.Franz@nasa.gov, (661)276-2022

Updated Miniature 3-Axis-Vibration High-Frequency Data Logger

Summary

The capabilities of a miniature, stand-alone system for acquiring high frequency vibration data were updated. The system was flown on Proteus and F-15B/836.

Objectives

Extend available recording time from minutes to hours, provide continuous recording capability, extend range of operating conditions (temperature, pressure, and vibration) that the recorder itself can withstand.

Justification

The original data logger was developed by the Flight Instrumentation Branch for quick installation in aircraft areas in order to quantify the actual vibration environments in those areas and thereby provide data to developers who need to flight qualify scientific instruments. The system was successfully used on B-52B/008 and F-18/845. Then requirements for enhanced capabilities arose.

Approach

The ambient temperature range that the system could operate in was extended to -40°F by the addition of a glue-on polyimide heater on the hard drive. The data logger measured the drive's temperature and controlled the heater. Longer recording times were achieved by using a larger capacity hard drive (512 MB). Continuous recording was achieved by reducing the sample rate somewhat and using a double-buffered memory scheme. A combination of hardware and software changes also resulted in a system noise level reduction. Commercially-available software was also acquired to automate data offloading.

Status

The updated system was flown on a new pod developed for the Proteus aircraft to carry scientific instruments. It was also flown on F-15B/836 to quantify the vibrations that were thought to be causing problems with certain research equipment during supersonic flight.



Photograph of data logger (tall box), optional control box, and three-axis accelerometer.

At the time of this writing, a solid state hard drive has been installed in the system and is expected to extend both the altitude and the rate of change in altitude that the system can tolerate. Likewise the solid state hard drive is expected to increase the vibration level that the system itself can withstand.

Contact

Philip.J.Hamory@nasa.gov, (661)276-3090

Reference

Miniature 3-Axis-Vibration High-Frequency Data Logger, 2000 Research Engineering Annual Report, Phil Hamory, RI. (also available as NASA/TM-2004-212025)

Specifications of Present Configuration

Full Scale Range	+/- 75g
Resolution	0.036g
Noise Level	$7 \times 10^{-6} \text{ g}^2/\text{Hz}$
Accuracy	+/- 10% (*)
Sample Rate	7,000 Hz
Frequency Response	2 Hz to 2000 Hz
3-pole Butterworth anti-aliasing filter cutoff frequency	3000 Hz
1-pole AC coupling filter cutoff frequency	1.6 Hz
Accelerometer	Endevco 5253A-100

(*) The main limitations are cross-axis sensitivity and frequency dependence of the accelerometer chosen.

Recording Time	3 hours
Recording Medium	rotating hard drive or solid state hard drive
Size	6.425" (L) x 4.350" (W) x 4.700" (H) as shown in photo
Weight	3 pounds
Power Consumption	250 mA @ 28V 1A @ 28V with heater on rotating drive
Temperature	-40 °F to 185 °F
Altitude	up to 50,000 ft (with rotating drive) at least to 80,000 ft (with solid state drive)
Vibration	System passed DFRC Process Spec 21-2 Curve B with the rotating drive; higher capability expected with solid state drive

Relative Navigation Technique to Support the Development of a Refueling Drogue Model

Summary

The Automated Aerial Refueling (AAR) Project gathered data desired to develop a model of refueling hose/drogue behavior--particularly under the influence of the receiving aircraft forebody. The trailing pilot needed to fly in positions relative to the lead aircraft's refueling drogue. In order to position the pilot of the trailing (receiving) aircraft properly, a relative navigation system was developed that provided the trailing pilot with guidance needles. Pre-set coordinates could be dialed in by the trailing pilot (using BCD switches) so that the needles would center when positioned at the appropriate x,y,z coordinates relative to the lead aircraft.

The Airborne Information Management System (AIMS) was used to process data from research-grade GPS receivers. The AIMS is a Dryden in-house developed system that has been used on a number of Dryden research aircraft. The GPS position of the lead aircraft was transmitted to the trailing aircraft. There, data was time-aligned with the trailing aircraft GPS position data, adjusted for latency, and the relative position between them was computed. The lead aircraft heading was used as the formation heading, and the relative position of the two aircraft along the formation heading was computed and displayed to the trailing pilot on the HUD. A similar system was used on the Autonomous Formation Flight (AFF) Project--except the direction of information flow was reversed, the formation heading was the lead aircraft heading (instead of being fixed), and the system was programmed to handle a different piloting technique.

The drogue mapping activity required the trailing pilot to fly at preselected positions relative to the leading aircraft refueling basket (drogue). Pre-set tables were programmed into the trailing aircraft AIMS, and small horizontal adjustments could be made by pilot inputs on a stick switch.

Objective

GPS absolute position accuracies that are not differentially corrected can exceed 100 ft in error. By subtracting nondifferential positions of two GPS receivers in the same airspace, AFF and ARR demonstrated that most of the common error sources can be cancelled out, leaving a residual relative spacing error of just a few feet. This greatly simplified the design of the required system. Another unique feature of the pilot display is that it creates a "virtual" 10 sample-per-second needle update from GPS data that only outputs twice per second. This yields a more smooth update to the needles. The downside of this algorithm is that the formation must be on a constant heading for the extrapolation to work properly. However, since this was a constraint on the test condition, it was not a problem.

Status/Plans

The AAR drogue model study flight test has been completed. Should the two F18s (tail numbers 845 and 847) be required for other research activities, the AIMS and GPS receiver hardware can be reprogrammed to support those missions.

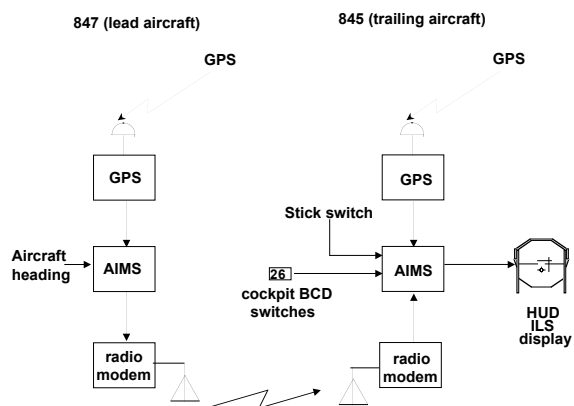


Figure 1. Simplified block diagram of the GPS relative navigation system.

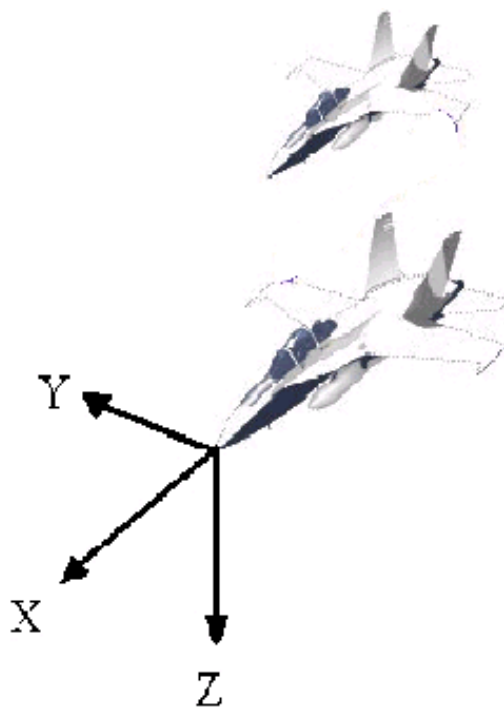


Figure 2. Formation Coordinate System.

Contacts

Glenn Bever, NASA Dryden, Code RI, x3747

Curtis Hanson, NASA Dryden, Code RC, x3966

Development of STARS Phase 2 Range User System Flight Hardware

Summary

Current space launch vehicles utilize remote ground stations for telemetry data relay and range-safety. These remote sites are costly to operate and maintain. NASA's Space-Based Telemetry and Range-Safety Study (STARS) is investigating the use of space-based data relay and range-safety for Next Generation Launch Technology (NGLT) vehicles.

The Phase-1 STARS study involved implementing a range-user (RU), telemetry, data system similar in architecture to current launch vehicle high rate data systems and flying it aboard an F-15B test aircraft. These flights made it possible to characterize system performance on a high dynamic vehicle and will serve as a baseline of comparison for results from Phase-2.

The STARS Phase-1 Range User system consisted of a data multiplexer that accepts analog video, voice, pseudorandom data and IRIG-B time inputs. The video and voice signals were digitized, compressed, and then multiplexed with the pseudorandom data and IRIG time to create a standard IRIG-106 data stream. The format was programmable at 125kbps, 250kbps or 500kbps for a given test flight and the compressed video was only included in the 500kbps format.

This data was transmitted to the Tracking and Data Relay Satellite System (TDRSS) using a Quadrature Phase Shift Keying (QPSK) modulated transmitter and power amplifiers that feed two omni-directional Right Hand Circular Polarized (RHCP) patch antennas on the top and bottom of an F15B test aircraft. This system implementation is similar in architecture to current expendable launch vehicle (ELV) high rate data systems and was tested on the F15B aircraft in order to characterize performance on a high dynamic vehicle. The STARS Phase-1 Range User and Range Safety systems performed in accordance with predictions and met Phase-1 flight demonstration goals.

Phase-2 of the RU System STARS study will develop the hardware required to implement a reliable space-based high data rate communication link and demonstrate an order of magnitude increase in data transmission rates compared to present day systems.

Objective

The baseline Range User system performance for current ELVs is inadequate in two areas. First, the data rate that can be achieved with an omni-directional antenna is limited due to the free space loss involved in satellite transmission. The preferred option to increase the data rate would be the use of a phased array antenna system. Second, the link implemented for the first flight demonstration was a standard IRIG-106 data link. The preferred option for future satellite telemetry data links would be an Internet Protocol (IP) based link allowing uplink command and control, real-time changes in data format and repeat requests of corrupted data.

The primary Range User system objective for the STARS Phase-2 is to increase the achievable data rates through the development of improved data transmission hardware. The greatest weakness in current satellite telemetry systems is the vehicle transmit antenna. Currently most reusable launch vehicles (RLVs) and ELVs utilize multiple omni-directional antennas. These systems may be supplemented by switching hardware to direct transmitter power to the antenna pointed at the receive satellite, however, they are limited by the transmitter power available and low gain antenna utilized. Unmanned Aerial Vehicles (UAVs) often make use of steerable dish antennas to achieve higher gain

and therefore greater data rates. However, these systems result in the requirement for a radome well above the vehicle surface resulting in thermal problems for launch vehicle applications or limited look angles if recessed in the vehicle.

Status/Plans

The RU system under development includes an IP data system, Ku-band transmitter and phased array antenna system. Two transmitter systems are being developed; one based on existing TDRS-4 transmitter hardware and a second utilizing low cost hardware developed specifically for STARS Phase-2 flights in an effort to reduce the cost of future satellite communications systems. The phased array antenna, Figure 1, utilizes on-board GPS/INS and an antenna controller to point the antenna to a selected satellite. Development and optimization of this and future antenna control system is another goal of the RU Phase-2 system development.

Procurement of all required hardware for the flight test has been initiated. Integration on the test aircraft will begin 2004. Satellite compatibility testing of the transmitter hardware will also be conducted in 2004. Phased Array Antenna systems tests were conducted in late 2003 and tests with the INS/GPS interface were conducted early in 2004. The STARS Phase-2 flight test demonstration will be conducted at DFRC in FY2005.

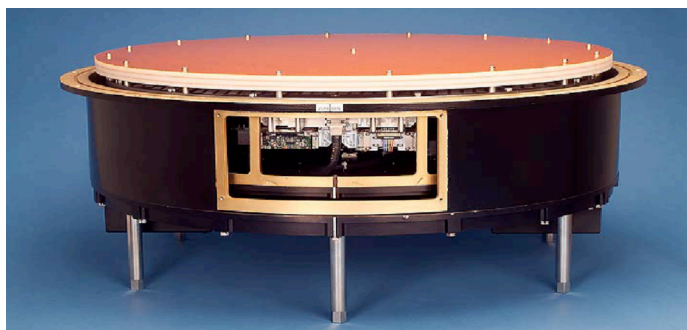


Figure 1. Phased-Array Antenna with Radome Removed.

Contacts

Robert Sakahara, NASA Dryden, Code MC, x2566

Don Whiteman, NASA Dryden, Code RI, x3385

Russ Franz, NASA Dryden, Code RI, x2022

Flight Tests of Phase-1 Space-Based Telemetry and Range-Safety Study

Summary

Current space launch vehicles utilize remote ground stations for telemetry data relay and range-safety. These remote sites are costly to operate and maintain. NASA's Space-Based Telemetry and Range-Safety (STARS) Study is investigating the use of Space-based data relay and range-safety for Next Generation Launch Technology (NGLT) vehicles, Figure 1.

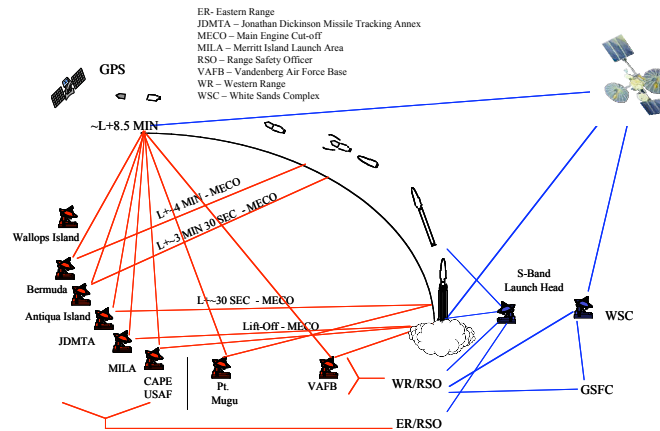


Figure 1. Current versus NGLT Data Relay.

Several NASA centers including KSC, GSFC, and DFRC are involved in the development and flight test of hardware to support NGLT Reusable Launch Vehicle (RLV) requirements. DFRC is responsible for the development of the range-user (RU), telemetry, data relay system, aircraft integration, and flight testing of both the range-user and range-safety (RS) systems.

Objective

The primary objective of STARS is to demonstrate the capability of space-based data systems to provide RS and RU functions. This should result in a significant cost savings due to reductions in ground-based assets required to support NGLT RLVs.

The STARS project will also develop new satellite communications component technologies. This will enable the implementation of space-based RS as well as RU systems that will support data rates that are an order of magnitude higher than current ELV systems.

Status/Plans

Phase-1 flight tests of the STARS RS and RU hardware were completed at DFRC in FY03. The flights were conducted on an F15B aircraft in order to simulate the type of dynamic environment in which a range safety system would be required to operate, Figure 2.

The Phase-1 flights utilized a RS satellite transceiver with a 400bps forward link for simulated space-based flight termination commands. The RS system also included a 10kbps satellite return link to provide system health, status and position information. Phase-1 testing incorporated a launch-head, similar to that implemented at current launch sites, to supplement the satellite based data relay system during the initial launch phase.

The Phase-1 RU system operated at 125, 250 and 500kbps in order to characterize the performance of current RU data systems. The RU system was a return link only system and didn't utilize the launch head.

The flight demonstration satellite data relay was via Tracking and Data Relay Satellite System, (TDRSS), White Sands Complex (WSC), NASA Integrated Services Network (NISN) to the DFRC Mission Control Center (MCC). The DFRC Aeronautical Test Facility (ATF) was modified to support RS uplink/downlink operation as the launch head.



Figure 2. Integration of STARS RS and RU Systems.

The STARS flight tests successfully demonstrated the capability of a space-based range safety system to provide a reliable flight termination link in a dynamic environment. The RU system performed as predicted and the data collected and operational lessons learned are being utilized as guidelines for the development of improved hardware.

Enhanced RS and RU systems are currently being developed for Phase-2 flight tests in FY05. The improvements include integration of the RS system components into a single flight unit as well as RU system antenna and transmitter development to support data rates that are an order of magnitude higher than current RLV systems.

Contacts

Robert Sakahara, NASA Dryden, Code MC, x2566

Don Whiteman, NASA Dryden, Code RI, x3385

Howard Ng, NASA Dryden, Code RI, x3803

Keith Krake, Spiral Technology, Code RI, x2147

Flight Tests of Enhanced Flight Termination System (EFTS)

Summary

The Enhanced Flight Termination System (EFTS) Program goal is to develop the next generation flight termination system for Department of Defense and NASA Ranges. The program will address robust command links for flight termination including message formats, modulation methods, and encryption. The scope and specific objectives of the program are summarized below; some objectives have been combined for clarity:

- Security, including protection against unintended commands, and selectable termination for simultaneous multiple operations
- Use of the existing radio frequency spectrum and other frequency bands
- Minimal impact to existing ground and airborne (including failsafe) equipment
- Minimal impact on transmission and processing time (latency)
- Mature and develop reliable technologies and design solutions
- Immunity to interference from (authorized) operating signals in Flight Termination System (FTS) band (see also RCC task FM-31)
- Increase number of vehicles supported by a FTS frequency

The program has been segmented into three parts: (a) Part 1 was the Range Commanders Council (RCC) – Range Safety Group (RSG) study that investigated the objectives identified above. (b) Part 2 is a two-phase effort, Phase I built prototype enhanced flight termination receivers (FTR) and encoders to undergo factory test, integration test, and flight test. Phase II will develop the final flight and ground hardware for implementation. (c) Part 3 will implement the EFTS ground encoders on the ranges that require FTS. Implementation will be dependent upon funding availability. This flight test supported Part 2 – Phase I of the EFTS Program.



Figure 1. NASA DFRC F-15B Aircraft.

Objective

The primary objective of the testing was to verify and validate the performance specifications developed during the EFTS study. This was accomplished by procuring prototype enhanced flight termination receivers (EFTRs) and encoder hardware, integrating the EFTS hardware in a lab environment, and then

flight-testing the EFTRs on a high dynamic vehicle, NASA DFRC F-15B aircraft, Figure 1. Lessons learned during the testing of prototype hardware provided information required for the development of production hardware requirements and operational procedures for Part 2 – Phase II.

Flight Test Results

The EFTS and an analog flight termination system (FTS), Figure 2, were installed on the F-15B aircraft for flight tests in late FY03. Several flight tests were conducted and it was demonstrated that the prototype EFTS performed as well as the analog system and no operational problems were encountered.

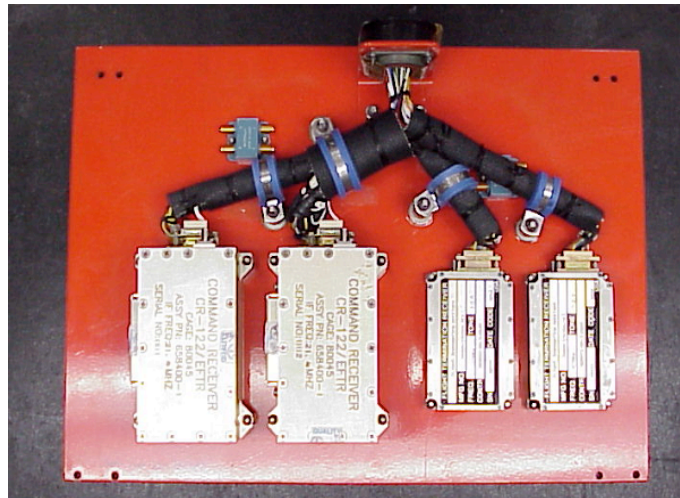


Figure 2. Enhanced and Analog FTRs.

Based on the successful bench and flight test results for EFTS, the requirements document for future operational systems was developed. The flight testing conducted on the high dynamic NASA F-15B helped to further prove that the design would function in an operational environment. Modifications to the design specifications and digital command link message format were made as a result of the flight tests and laboratory testing.

Contacts

Robert Sakahara, NASA Dryden, Code MC, x2566

Don Whiteman, NASA Dryden, Code RI, x3385

Howard Ng, NASA Dryden, Code RI, x3803

Dryden Aerospike Rocket Test

Summary

Although the advantages of the aerospike nozzles are well understood through analysis and ground testing, the lack of flight test data has precluded use of these nozzles in the current generation of space launch vehicles.

In the Dryden Aerospike Rocket Test project, flight research of aerospike rocket nozzles was conducted using high-power amateur rockets. High-power amateur rockets provided a convenient, inexpensive testbed to conduct aerospike flight research. The conventional nozzles in these rockets were replaced by aerospike nozzles, and the instrumented rockets were flown with aerospike nozzles.

Objective

The main objective of the current research is to measure the in-flight performance of aerospike nozzles using high-power amateur rockets.

Justification

The aerospike rocket nozzle has been shown to have significant advantages over the conventional bell nozzles for advanced space transportation systems. Figure 1 demonstrates the performance advantage that an aerospike nozzle has over a conventional nozzle with the same area ratio. The solid line and the data points are the nozzle efficiencies of the aerospike nozzle tested by Rocketdyne in the 1960s, and the dotted line is the nozzle efficiency of a conventional bell nozzle. Ground test data indicated that the Dryden Aerospike Rocket Test nozzle has an efficiency of approximately 97% as shown in figure 1. Built-in altitude compensation allows an aerospike nozzle to operate at near optimum expansion ratio from sea level to orbital insertion. The aerospike nozzles also make better use of a launch vehicle's base, and they are shorter than a conventional nozzle. Proposed uses for the aerospike nozzles included the Saturn-class rockets, space shuttle main engine, X-33, and VentureStar. But the lack of flight data has hindered the use of these nozzles on actual space launch vehicles.

A comprehensive flight test data base and, preferably, actual rocket launches with aerospike rocket motors are required before these nozzles can be seriously considered for actual application on space launch vehicles.

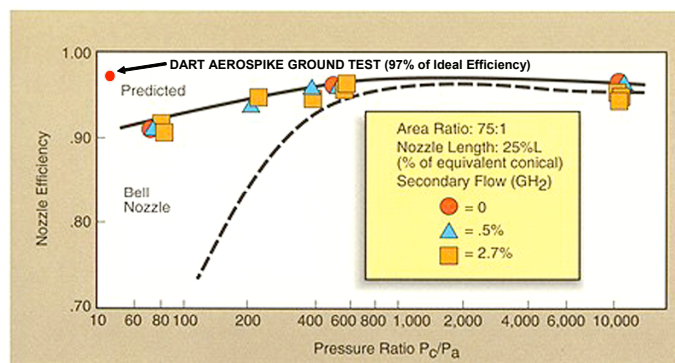


Figure 1. Performance advantage of the aerospike nozzles.

Approach

The flow path design for the aerospike nozzles was done at NASA Dryden in collaboration with the Air Force Flight Test Center. Blacksky Corp. designed and fabricated the rocket testbed vehicle. Blacksky Corp. also coordinated development of the experimental aerospike nozzles and solid propellant motors used in the tests with Cesaroni Technology Inc. One conventional conical nozzle and three aerospike nozzles were test-fired on the ground. Two aerospike rockets were flown successfully on two consecutive flights on March 30 and 31, 2004 at the Pecos County Aerospace Development Corporation Flight Test Range in Fort Stockton, Texas. The rockets reached supersonic speeds in excess of Mach 1.5 and peak altitudes of more than 26,000 ft. A third planned rocket launch using a conventional nozzle was postponed due to bad weather. Preliminary data analysis showed high aerospike nozzle efficiencies in flight.



Figure 2. Dryden aerospike rocket flight number 1.

Contact

Trong Bui, Code RP, (661) 276-2645,
trong_bui@mail.dfrc.nasa.gov

C-17 Propulsion Health Monitoring

Introduction

Future military and commercial aircraft turbine engines must be safe and affordable to maintain America's pre-eminence in the aerospace market. To address these needs, NASA Dryden Flight Research Center (DFRC), NASA Glenn Research Center (GRC) and Pratt & Whitney (P&W) have formed a team to plan and execute a flight test research project in the area of propulsion system prognostics and health monitoring. The goal of the overall proposed program is to define, flight-demonstrate, mature and refine integrated propulsion health monitoring (PHM) system technologies for civil and military transport aircraft. A PHM system targeted towards transport aircraft will extend the capabilities of health management systems being demonstrated on the F/A-22 aircraft and use advanced prognostic sensors and intelligent reasoning software being developed for the Joint Strike Fighter. In addition, NASA and industry are jointly developing new sensor technologies and data fusion algorithms for the PHM flight demonstration.

The PHM system has been implemented aboard the USAF C-17A aircraft T-1 (See fig. 1) The experimental sensors are installed on engine #3.



Figure 1. USAF C-17A aircraft T-1.

Objectives

This flight test effort has multiple objectives. The primary objective of this research is to evaluate sensor suites in the flight environment and if possible, bring them up from their current status of promising laboratory technology to being reliably available for use in the flight environment. The goals and objectives for each individual sensor test activity are elaborated in more detail below. Figure 2 shows the location of each sensor around the engine.

1. The Inlet Debris Monitoring Sensor IDMS sensor is a coordinated pair of conductive strips installed on the inlet forward of the first (1st) stage fan blade. This sensor monitors the electrostatic charge associated with debris ingested at the engine inlet. It is designed to detect the size, quantity, velocity, and to a limited extent, composition of debris (i.e. damaging/non-damaging) entering the inlet.
2. The Engine Distress Monitoring System (EDMS) is installed in the upper actuator housing of the thrust reverser casing. This sensor monitors the electrostatic charge of debris exiting the engine. The intent is to monitor the exhaust for changes in the level or nature of this debris.

3. The Stress Wave Analysis (SWAN) sensor is a lightweight integrated circuit piezoelectric transducer that monitors structurally borne ultrasonic sound vibrations to measure the energy created by shock or friction events. It is an external sensor that requires a mount point that provides a mechanical sound path to the component being monitored. For this test, five (5) SWAN sensors will be mounted on the engine gearbox and flanges.
4. A set of six (6) high frequency vibration sensors (HFVS) are mounted on the engine. Four (4) will be located on the gearbox (gearbox hi and the triaxially mounted set of three accelerometers), one (1) on engine case flange B (forward) (B-flange hi), and one (1) on flange P (aft) (P-flange hi). The B- and P-flange accelerometers are supported by two (2) lower frequency accelerometers, B-flange low and P-flange low. The goal is to characterize the high frequency response of components of the engine and gearbox. The frequency ranges being monitored include that of the ball and blade passing, tower shaft, Permanent Magnetic Alternator (PMA), idler gear and oil pump gear. Figure 3 shows sample power spectral densities from the accelerometers on the B-flange and the gearbox.

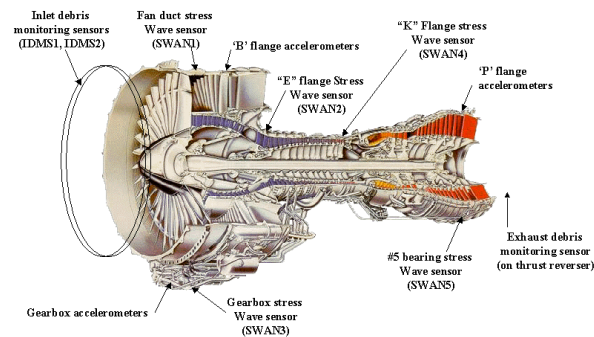


Figure 2. PHM sensor location on Pratt & Whitney PW2040 series turbofan, F117-PW-100.

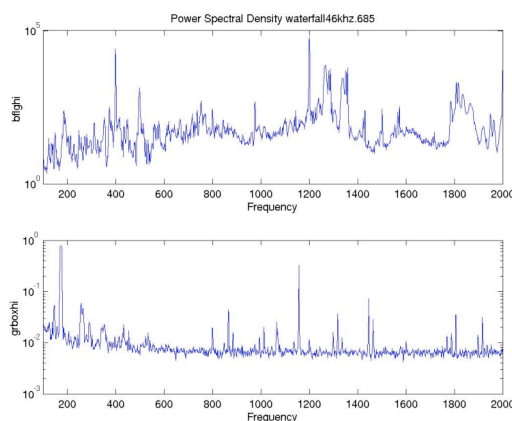


Figure 3. Power Spectral Density of B-Flange hi and Gearbox hi.

Contacts

Trindel Maine, Kimberly Ennix, Glenn Bever, Mike Venti, Art Ortiz

Carbon Composite Control Surface Test Program

Summary

The NASA Dryden Flight Loads Laboratory (FLL) completed the first phase of thermal / mechanical testing for the Next Generation Launch Technology (NGLT) Ceramic Matrix Composite (CMC) Control Surface test program. During this phase, a subsection of a proposed ACC carbon-carbon (C/C) control surface (56 in. long x 39 in. wide) was subjected to combined thermal / mechanical loads to verify the structural adequacy of the design while René 41 attachment rings simulated the vehicle to control surface interface. Based on previous room-temperature testing, the original C/C torque tube was redesigned to incorporate carbon-silicon carbide (C/SiC) and a new load transfer methodology.

The control surface was integrated into the FLL inert chamber and subjected to combined National Aerospace Plane (NASP) design limit load (DLL) conditions ($\pm 8490 \text{ lbf}$) along with single and dual sided X-37 bodyflap heat loads (max. 2000°F). Mechanical loading was introduced along the trailing edge of the control surface while quartz lamp heaters were used to heat both the windward and leeward surfaces. At temperatures above 550°F , the chamber was purged with nitrogen to achieve levels of less than 0.02% oxygen during the tests.

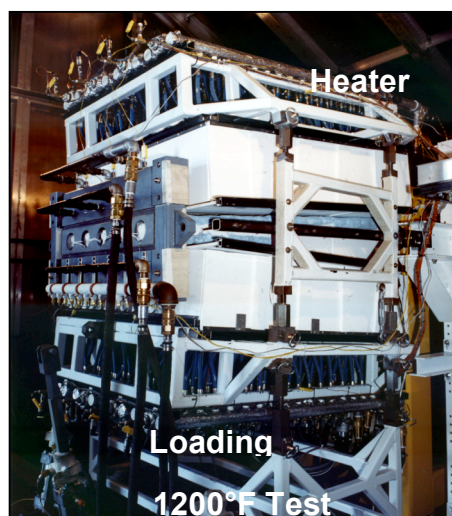
A total of 54 strain sensors, 50 thermocouples, and 6 deflection sensors were integrated onto the control surface. The strain sensors consisted of both conventional wire resistive strain gages (40 total) and EFPI fiber-optic strain sensors (14 total). In addition, a newly developed optical temperature measurement technique demonstrated successful temperature monitoring up to 2000°F and correlated well with conventional thermocouples.

Objectives

- Verify the structural adequacy of a full-scale carbon-carbon control surface through thermal / mechanical testing.
- Develop test capabilities and techniques to validate future X-37 C/SiC control surfaces through thermal / mechanical testing.
- Obtain test data to validate thermal and structural analyses of X-37 C/C and C/SiC control surfaces.

Results

- Successful completion of room-temperature loading tests to $\pm 100\%$ DLL and combined thermal / mechanical testing to -100% DLL at 2000°F .
- Delivered all required data for analysis correlation.
- Established methods of testing oxidation sensitive CMC structures at high temperatures.
- Demonstrated successful optical strain measurements up to 1650°F .



Test Matrix for the Carbon-Carbon Control Surface.

Test Temp	Test Load	Chamber Atm.
Room-Temp.	+/- 8490 lb	Air
550 °F	- 2547 lb	Air
1200 °F	- 4245 lb	GN2
1650 °F	- 4245 lb	GN2
1650 °F (one side)	- 4245 lb	GN2
2000 °F	- 8490 lb	GN2
2000 °F (one side)	- 8490 lb	GN2

Contacts

Larry Hudson, Test Engr., DFRC, (661) 276-3925
 Craig Stephens, Test Engr., DFRC, (661) 276-2028
 Anthony Piazza, Instr. Spec., DFRC, (661) 276-2714
 Dr. Brian Sullivan, Project Engr., MR&D, (610) 964-6131

NGLT C/SiC Bodyflap Control Surface Test Program

Summary

The NASA Dryden Flight Loads Laboratory (FLL) completed the second phase of thermal / mechanical testing for the Next Generation Launch Technology (NGLT) Ceramic Matrix Composite (CMC) Control Surface test program. During this phase, a representative X-37 carbon-silicon carbide (C/SiC) bodyflap subcomponent (approx 24 in. long x 20 in. wide, 4 in. height; 4 in. diameter torque tube) was subjected to combined thermal / mechanical loads testing simulating X-37 re-entry conditions.

The control surface was integrated into the FLL inert chamber and subjected to combined subcomponent design limit load (DLL) conditions (370 lb_f) along with single sided X-37 bodyflap heat loads (max. 2060 °F). Mechanical loading was introduced along the trailing edge of the bodyflap while quartz lamp heaters were used to heat the windward surface. A cold plate, maintained at 80 °F, simulated the leeward boundary condition. At temperatures above 550 °F, the chamber was purged with nitrogen to achieve levels of less than 0.02% oxygen during the tests.

A total of 27 strain sensors, 38 thermocouples, and 7 deflection sensors were integrated onto the control surface. The strain sensors consisted of both conventional foil strain gages (15 total) and EFPI fiber-optic strain sensors (12 total). Strain measurements were demonstrated to 1850 °F which raised the maximum temperature limit for EFPI strain sensors on CMC materials from 1650 °F. Over 95% of the instrumentation survived all testing.

Objectives

- Perform combined thermal and mechanical loading of a C/SiC bodyflap subcomponent.
 - Temperature time-histories based on X-37 heating.
 - Mechanical loads based on subcomp. design limit load.
- Demonstrate, through test, the technologies associated with joining separate CMC control surface segments.
- Provide valid temperature, strain, and deflection data for correlation with analyses.

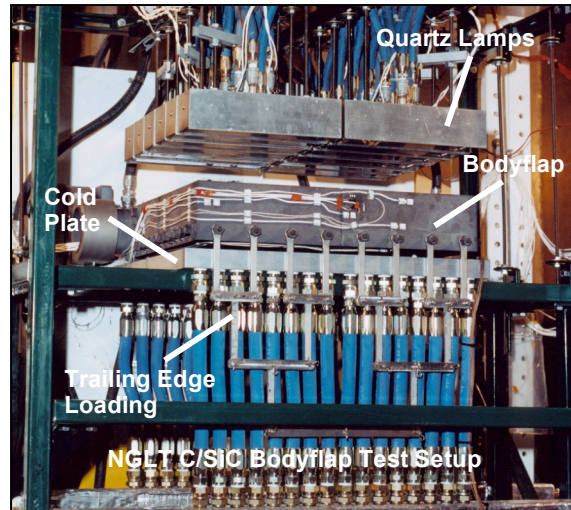
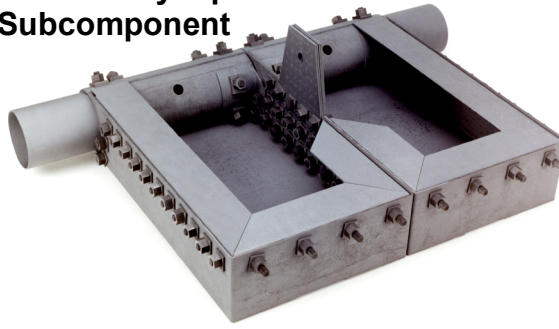
Results

- Successful completion of ten tests, including six combined thermal / mechanical tests to 2060 °F and 100% DLL.
- Delivered all required data for analysis correlation.
- Continued refining methods of testing oxidation sensitive CMC structures at high temperatures.
- Demonstrated successful optical strain measurements up to 1850 °F.
- Demonstrated “Virtual Flight Loads Lab” system by broadcasting real-time test data and video to customer’s desktop.

Contacts

Larry Hudson, Test Engr., DFRC, (661) 276-3925
Craig Stephens, Test Engr., DFRC, (661) 276-2028
Anthony Piazza, Instr. Spec., DFRC, (661) 276-2714
Dr. Brian Sullivan, Project Engr., MR&D, (610) 964-6131

NGLT Bodyflap Subcomponent



Test Matrix for the NGLT C/SiC Bodyflap.

Test ID	Test Load (%DLL)	Test Temp (°F)	Chamber Atm.	Comments
1	50	Room	Air	
2	100	Room	Air	Max load (370 lb _f)
3	0	550	Air	Heating System Check
4	100	550	Air	Load then Heat
5	100	1200	Nitrogen	Load then Heat
6	100	1650	Nitrogen	Load then Heat
7	100	2059	Nitrogen	Load then Heat (repeated twice)
8	100	2059	Nitrogen	Heat then Load (data sensitivity to heat first)

X-37 Hot-Structure Control Surface Development Program

Summary

The development of hot-structure control surfaces for the X-37 has been identified as a high-risk technology. Hot-structures are required for both the X-37 flaperons and ruddervators and to mitigate risk; NASA / Boeing have initiated a program to develop X-37 hot-structures using carbon-carbon (C/C) as well as carbon-silicon carbide (C/SiC) technology.

The NASA Dryden Flight Loads Laboratory (FLL) and the Air Force Research Laboratory (AFRL) at Wright-Patterson AFB are responsible for the thermal / mechanical testing of both the X-37 flaperons and ruddervators. NASA Dryden will be responsible for X-37 flaperon testing while AFRL will be testing the X-37 ruddervators. Between March 2004 and July 2005, both laboratories will be subjecting C/C and C/SiC subcomponent and qualification unit test articles to thermal and mechanical load conditions simulating X-37 re-entry conditions.

The X-37 flaperons will be integrated into the FLL inert chamber and subjected to the required mechanical design limit load (DLL) conditions. Mechanical load introduction will be either along the trailing edge for the C/SiC flaperon or distributed, using load pads, for the C/C flaperon. Mechanical testing will be to 100% DLL for both the subcomponent and qualification units.

For thermal testing, quartz lamp heaters will be used to heat the flaperon windward surface while other boundary conditions will be simulated as required (insulated, cold plate, etc.). At temperatures above 550 °F, the chamber will be purged with nitrogen to achieve levels of less than 0.02% oxygen during the tests. Thermal testing will be to a maximum temperature of 2400 °F for the subcomponent tests and to approximately 2700 °F for the qualification units.

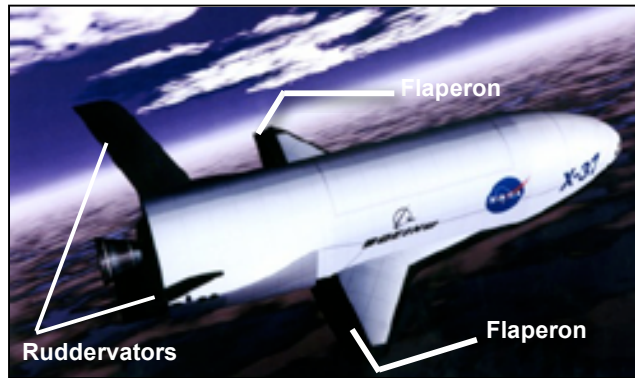
Strain sensors (both foil and fiber-optic), thermocouples, and deflection sensors will be integrated onto the flaperons. Fiber-optic strain measurements will be obtained to 1850 °F.

Objectives

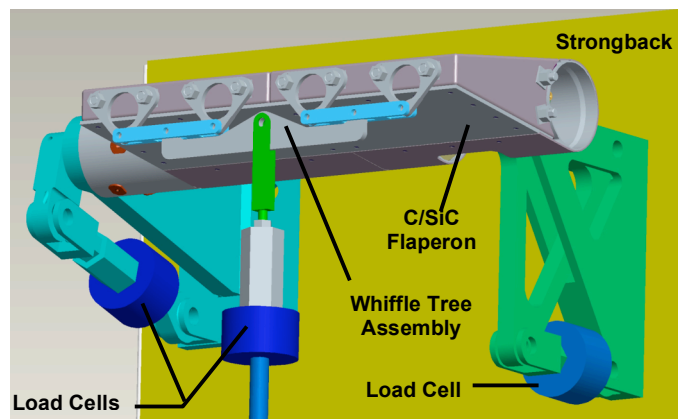
- Perform thermal and mechanical testing of X-37 C/SiC and C/C flaperon subcomponent and qualification units.
- Demonstrate, through test, the technologies associated with the development of ceramic matrix composite control surfaces.
- Provide valid temperature, strain, and deflection data for correlation with analyses.

Contacts

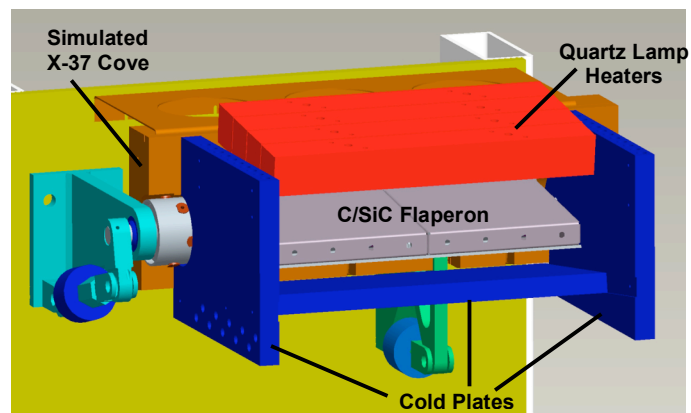
Larry Hudson, Test Engr., DFRC, (661) 276-3925
Craig Stephens, Test Engr., DFRC, (661) 276-2028
Anthony Piazza, Instr. Spec., DFRC, (661) 276-2714
Larry Chien, Test Design, AS&M, (661) 276-5803
Robert Shannon, Test Engr., AS&M, (661) 276-2231



X-37 C/SiC Flaperon Subcomponent.



Room-Temperature Mechanical Test Set-Up.



Thermal Test Set-Up.

NASA Dryden “Virtual Flight Loads Lab”

Summary

In an effort to enhance the testing capabilities of the NASA Dryden Flight Loads Laboratory (FLL), personnel set out to develop a communication enhancement tool to support both FLL customers as well as educational outreach goals. The results were the development of the “Virtual Flight Loads Lab” (VFLL) which provides “data-at-the-desk” capability.

FLL personnel utilized commercial-off-the-shelf (COTS) software to develop the VFLL as a tool that allows near real-time transmission of both data and video to off-site locations. Some of the key features of the VFLL are as follows:

- The use of COTS software allows for easy application of the VFLL at remote locations.
- Data transmission is encrypted (up to 256 bits) and only viewable using secure decryption keys.
- Modifications to the FLL audio communication systems allow customers / students the ability to actively monitor and participate in an ongoing test.

In November 2003, the VFLL was successfully used to conduct a near real-time broadcast (200 msec delay) of a thermal / mechanical test of a NGLT carbon-silicon carbide bodyflap simultaneously to NASA Langley and to a remote site at NASA Dryden. A total of 1024 channels of data and 4 video streams were broadcast during the demonstration.

The VFLL has also been developed as an education outreach tool to allow students the ability to actively participate and observe testing in the FLL. Combined with teaching modules, the VFLL provides teachers with an effective tool to enhance in-class learning. In June 2003, the educational benefits of the VFLL were demonstrated when a FLL test was broadcast live to a 6th grade class at Joe Walker Middle School in Quartz Hill, Ca. FLL personnel participated in both the test operation and in-class instruction.

Objectives

- Develop a cost-effective means of maximizing customer participation in FLL test activities.
 - Save time and money while simultaneously increasing productivity.
- Develop an educational outreach tool that can be inexpensively utilized by K-12 schools as well as universities.

Results

- The VFLL has been demonstrated as a cost-effective tool to maximize customer and student participation in FLL test activities.

Contacts

Allen Parker, Meas. Engr., DFRC, (661) 276-2407
Larry Hudson, Test Engr., DFRC, (661) 276-3925
Craig Stephens, Test Engr., DFRC, (661) 276-2028
Anthony Piazza, Instr. Spec., DFRC, (661) 276-2714

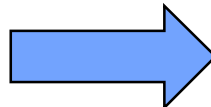
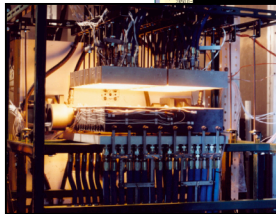
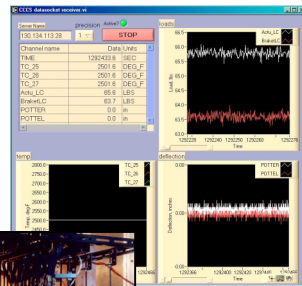
**NASA Dryden
Flight Loads Laboratory**



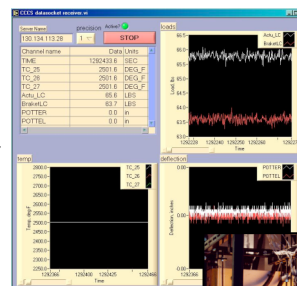
Desktop at Customer's Site or School



**Connection
to Lab Com
System**



**Near Real-Time Data &
Video Transfer
Via The Internet
(Encrypted Data)**



Fiber Optic Sensor Attachment Development and Performance Evaluations

Summary

Aerostructures Branch personnel at NASA Dryden have been evaluating and characterizing fiber optic (FO) based strain and temperature measurements for over seven years. Research conducted in the Flight Loads Laboratory (FLL) has subjected FO sensors to hostile environments for in-flight applications and hot-structures ground testing (hypersonic). Sensor attachment of both fiber Bragg Gratings (FBG) and Silica based Extrinsic Fabry Perot Interferometers (EFPI) have been accomplished on metallic and composite substrates. These FO sensors, depending on the application, are currently being evaluated:

- at room and elevated temperatures
- with combined applied thermal / mechanical loads
- and on large-scale structures for ground testing

Objectives

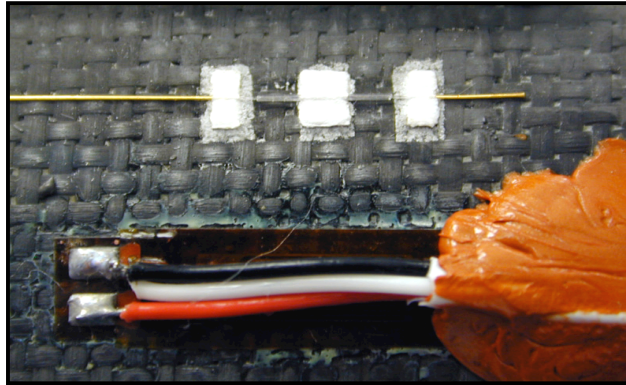
Develop attachment techniques and evaluate FO strain / temperature sensor performance for Structural Health Monitoring aerospace applications. Sensor evaluation tasks include:

1. Develop attachment techniques of EFPI sensors on both carbon-carbon (C-C) and carbon-silicon carbide (C-SiC) substrates for high temperature applications.
2. Evaluate EFPI sensor performance from room-temp to 1650 °F, under thermal and combined thermal / mechanical loads.
3. Determine maximum operating temperatures of EFPI for X-37 hot-structures program.
4. Begin working on Sapphire sensors for strain measurements beyond the temperature limits of the Silica EFPIs.

Results

An eight-foot long 130 FBG fiber (0.5-in grating spacing) was attached to a two-foot square graphite-epoxy composite panel. In addition 12 EFPI strain sensors were calibrated for embedment into the composite panel during fabrication. The panel was then loaded in the FLL Shear Load Fixture. Excellent indicated-strain correlation of the FBG's with respect to collocated conventional foil strain gages was achieved. Also, the embedded EFPI sensors measured within 5% of its respective reference foil strain gages.

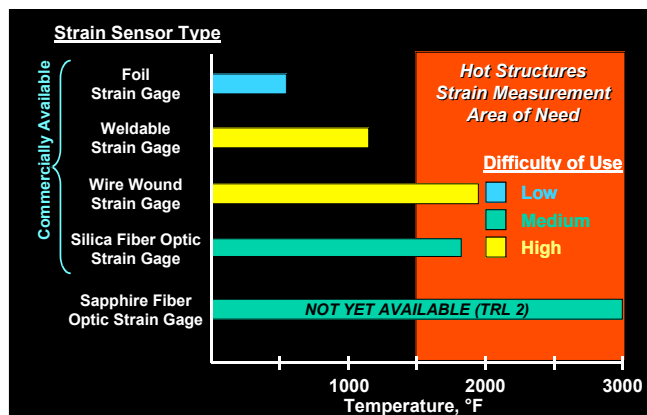
Thermal-spray attachment procedures were also developed for the EFPI sensors on C-SiC substrates. High-temp installations were completed, including 14 EFPIs, on a C-SiC bodyflap (NGLT program) instrumented for ground testing in the FLL. Testing was completed to 100% Design Limit Load and 2050 °F in an inert Ni atmosphere chamber. The EFPI sensors were operational beyond 1850 °F. Only one EFPI sensor failed during testing.



Close-up of EFPI sensor and foil strain gage on NGLT Bodyflap torque tube.

Dilatometer tests were performed on C-SiC substrates instrumented with EFPI strain sensors to evaluate / characterize sensor performance. These tests verified that substrate expansion correlated well with interferometer strain output and provided apparent strain correction curves for post-test analysis of NGLT bodyflap.

The chart below highlights the need for developing methods of obtaining strain measurements on hot-structures for hypersonic flight applications. The investigation into EFPI sensors on C-C and C-SiC substrates will continue, under OSP, NGLT, and the X-37 programs. In addition, work is underway to develop Sapphire based sensor technologies for operation in yet higher temperature environments, greater than 2500 °F.



Contacts

Anthony Piazza, DFRC, RS (661) 276-2714

Larry Hudson, DFRC, RS (661) 276-3925

Lance Richards, DFRC, RS (661) 276-3562

Craig Stephens, DFRC, RS (661) 276-2028

Data Decompositions and Nonlinear Identification for AAWAeroservoelastic Data Analysis

Summary

F/A-18 Active Aeroelastic Wing (AAW) aircraft data is used to demonstrate signal representation effects on uncertain model development, stability estimation, and nonlinear identification.

Objective

A fundamental requirement for reliable and robust model development is an attempt to account for uncertainty, noise, and nonlinearity, in particular, for model validation, robust stability prediction, and flight control system development. Data decomposition procedures are used for uncertainty reduction in model validation for stability estimation and nonlinear identification.

Approach

Data is decomposed using adaptive orthonormal best-basis and wavelet-basis signal decompositions for signal denoising into linear and nonlinear identification algorithms. Nonlinear identification from a wavelet-based Volterra kernel procedure is used to extract nonlinear dynamics from aeroelastic responses, and to assist model development and uncertainty reduction for model validation and stability prediction by identifying nonlinearity from the uncertainty.

Results

First and second-order kernels were extracted from AAW flight data at a flight condition of 15,000 ft, Mach number 0.85. The input was a multisine collective aileron sweep and the output was taken as accelerometer data from the forward right wing just inside the wing fold. Morlet filtering was applied and the filtered response with residual are shown in Figure 1.

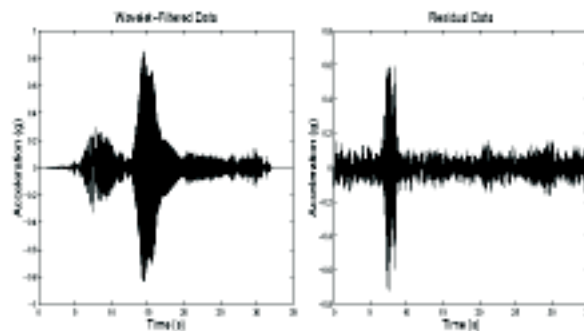


Figure 1. Morlet-filtered data and residual.

A first-order kernel was identified from the Morlet-filtered data, which was assumed to be linear. Then, a symmetric, secondorder kernel was extracted from the residual data, which was assumed to be composed of nonlinear data and noise. The identified kernels are shown in Figure 2.

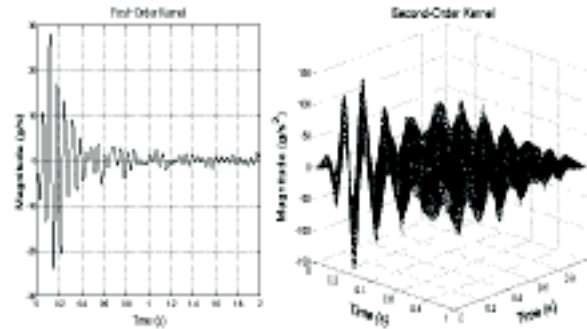


Figure 2. Identified first and second-order Volterra kernels.

The response predicted by the identified second-order kernel is depicted in Figure 3. The predicted second-order response is mostly concentrated in the 6 to 9 second time range. A detailed analysis of the residual data revealed significant 12 and 14 Hz responses corresponding to input frequencies of 6 and 7 Hz, respectively. This occurred in the time range of 6 to 9 seconds and is clearly indicative of a second-order nonlinearity. As shown in the zoomed-in plot in Figure 3, the second-order kernel is able to accurately predict this nonlinear response.

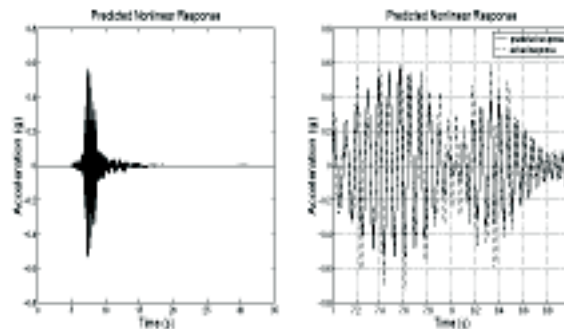


Figure 3. Nonlinear output predicted by the identified second-order kernel.

Benefits

Accurate linear and nonlinear estimation with adaptive data decompositions as pre-processing steps to the Volterra kernel representation. General applicability to any identification scheme.

References

- International Forum on Aeroelasticity and Structural Dynamics, Amsterdam, Netherlands, June 2003
- NASA/TM-2003-212021

Contact

Marty Brenner, x3793, Martin.J.Brenner@nasa.gov
 Chad Prazenica, rjp@gerc.eng.ufl.edu
 Aerostructures Branch, Code RS
 NASA Dryden Flight Research Center

48,000-Lb Capacity Aircraft Jack and Soft Support System (48K-3S)

Summary

A new ground test technique has been developed and is awaiting completion, to accommodate weight-and-balance measurements, complete inertia tensor measurements, ground vibration tests (GVT), control surface free-play tests and structural mode interaction tests (SMI) which all use one basic test setup. This new 48K-3S system saves time and money, and is safer from the standpoint that no critical lift is needed. The 48K-3S was designed and analyzed in 2001, 90% fabricated in 2003 and is now looking for funding to complete fabrication, assembly and ground test. Table 1 shows the cost savings to use the 48K-3S versus using the current method.

<i>Estimated Costs for the Current Soft Support Setup</i>			
Resource	Cost	Duration	Expense
Crane Rental	1000.00/day	7 days	7000.00
Critical Lift Crew of 24 people	900.00/person/day	2 days	43,200.00
		TOTAL	50,200.00
<i>Estimated Costs for the NEW Soft Support Setup</i>			
Resource	Cost	Duration	Expense
Critical Lift Crew of 5 people	900.00/person/day	0.5 days	2,250.00
		TOTAL	2,250.00

Table 1. Cost comparison for current and new 3S.

Current Test Setup

The current setup requires a crane lift of the aircraft being tested in order to slide three 3S assemblies beneath each aircraft jacking location. Each 3S weighs 1000 lbs and to center it exactly at the jacking location takes 4 people to muscle it into place. This means that at least 12 people are underneath the airplane (with the landing gear stowed) while it is suspended in the air. The aircraft is then lowered onto the three soft support assemblies (see Figure 1).



Figure 1. Current test setup for various ground tests.

The New 3S Design Philosophy

It was vital to eliminate the need for a critical lift and all the people that go with it to save time and money and to create a safer environment. It was also vital to easily transport and position the new 2500 lb system using one person. Therefore the system needed to easily roll under the aircraft while resting on its gear, be able to jack the airplane high enough to cycle and stow the gear, lower the airplane to a workable height and inflate the isolators. All this would take approximately 2 hours.

To eliminate the need for a critical lift the new 3S had to have an aircraft jacking capability. The “Direct Drive” (DD) worm gear driven electric cylinders were selected. The acme (vs. ball) screw model offers better performance in applications with long periods of no cylinder movement and heavy

vibration. The electric cylinder is an ideal substitute for hydraulic systems. Unlike hydraulics, electric cylinders consume energy only during operation. The electric motor drive eliminates the need for compressors, hydraulic tank, pressure control valves, pressure relief valves, directional control valves, hydraulic lines and fittings. Being self-contained, the electric cylinders need only to be “wired” to a control circuit. All mechanical components are enclosed inside a sealed, lubricating housing. A few safety features are the rotary limit switch with a mechanical stop that prevents overextension, the jacking speed designed to lift 3-4” per minute, an explosion proof brake motor that continues to brake if power is lost and an acme machine screw that prevents free play and back-driving when the system stops or starts from a stopped position. The base or platform that the electric actuators are mounted to was designed such that a heavy-duty pallet jack could be inserted three different ways underneath the base for various maneuvering options.

Figure 2 shows one of three identical assemblies used in the new 48K-3S. The large diameter cylinder in Figure 2 is the current isolator used for some GVT and SMI tests. All of the plate and block components were designed and fabricated in-house while the electric actuators, couplers, rods, mitre boxes, gear reducers and motors were purchased from a commercial source.

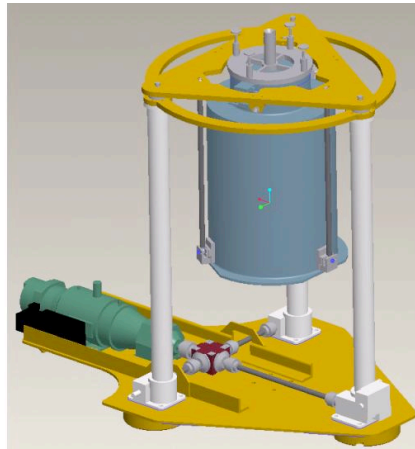


Figure 2. Pro Engineer model for 1 of 3 assemblies used in the new 48-K 3S.

Status/Plans

The assemblies are awaiting funding to buy material for the three top triangular plates see Figure 2 and paint. The 48K-3S is also lacking priority for assembly and proof load testing.

Contact

Starr Ginn, DFRC, RS, starr.ginn@nasa.gov

Creating Detailed Structural Dynamic Finite Element Models Using PATRAN

Summary

The structural dynamics group at NASA DFRC has a group of analysis and ground testing technologies that allow for confident decisions and high margins of safety. Our talents consist of Aeroservoelastic Modeling and Testing, Finite Element Modeling (FEM) that includes detailed structural dynamic modeling using IGES 3D solid model assemblies, structural dynamic equivalent beam models that are updated with a mode matching code using ground vibration test data and flutter analysis using the equivalent beam models. Our Ground Vibration Test (GVT) technology is up to date with industry and our testing methods and trouble shooting abilities have been improved over the last few years.

This summary describes one of our new abilities, which is the construction of finite element models (PATRAN/NASTRAN) using an IGES 3D solid model assembly. We have created detailed structural dynamic models for the B-52H Pylon, see Figure 1, and the X-37 Mockup or Drogue Chute Fixture (DCF), see Figure 2, which have been successfully verified with GVT results.

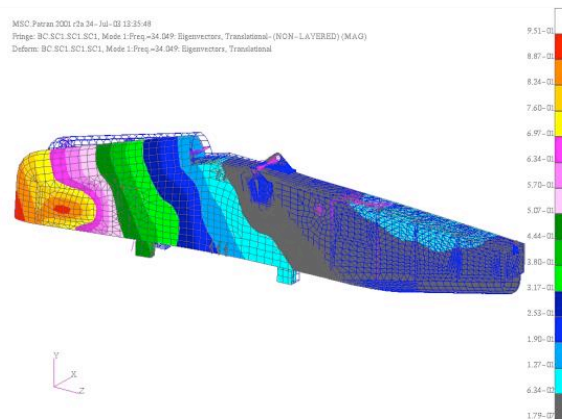


Figure 1. B-52H Pylon Detailed Finite Element Model.

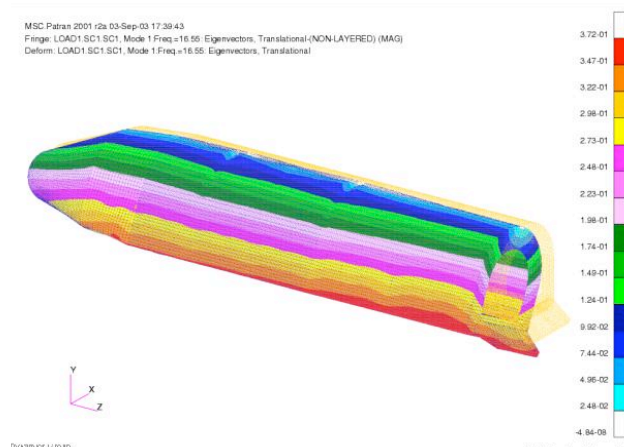


Figure 2. X-37-ALT Mockup Detailed Finite Element Model.

Objective

To produce good flutter results, a FEM and GVT are essential. Using only a FEM or only a GVT for the flutter analysis would be making bad assumptions. Even though the FEM alone is not perfect and the GVT alone is not perfect (test conductors make mistakes too), the FEM and the GVT together complete an accurate picture. Therefore, our objective was to create the finite element model from scratch, (if not supplied by the designer) to then be updated using the GVT results.

Creating a Detailed FEM using IGES Files

To create a FEM in the past one would have to refer to the designer's drawing, which makes for an extremely long process. Nowadays all designers use 3D modeling packages to create their designs. Most of these packages, including PATRAN, are capable of exporting and importing the assembly file as a type of universal file called IGES. The parts, which make up the assembly, can be exported as solids, surfaces or curves. Once the IGES file is brought into PATRAN the parts are separated into groups. Using the curves, for example, of the part in each group, a finite element model is created for that group. Once the curves have been used to create the FEM for each group of parts, the connections between all the FEM parts are created.

Using GVT Data for Model Validation

Accurately representing each connection point analytically is very difficult since you have to make an assumption for the stiffness of each connection. This is where the GVT results play an important role in updating the FEM. The GVT mode shapes become a guide to how the connection type or connection stiffness needs to be changed. On the other hand, the smoothness and phasing of the GVT mode shapes can be poor due to the GVT setup or curve-fitting technique used. For this situation the linearity of the FEM is used to create better GVT mode shapes by throwing out bad data and/or spending more time curve-fitting the frequency response functions.

Results

After reviewing the GVT mode shapes for the B-52H Pylon the only update made to the FEM was to decrease the stiffness between the pylon and where it connects to the B-52H wing. The GVT mode shape results for the DCF also changed only the connection stiffness between the DCF and the B-52H Pylon.

Status/Plans

Once the FEM connection points have been updated with GVT results, small stiffness and mass changes can be analyzed by the FEM only without repeating the GVT. This method will be used on the Propulsion Flight Test Fixture in 2004 where the experiment plans to fly several mass configurations/CG configurations.

Contact:

Starr Ginn, DFRC, RS, starr.ginn@nasa.gov
Chan-Gi Pak, DFRC, RS, Chan-Gi.Pak-1@nasa.gov

14,240-Lb Capacity Overhead Soft Support System (3S)

Summary

When performing a Ground Vibration Test (GVT) and/or Structural Mode Interaction (SMI) Test it is essential to decouple the test article from the ground to achieve a free-free environment, which most closely corresponds to flight. A soft support system (3S) is used to achieve this by inserting a very low frequency spring or isolator (< 1 Hz) between the test article and the ground connection point. Using a low frequency spring allows the modes of the test article to be isolated from the effect of being on the ground.

The cheapest way to construct a 3S is to hang the test article from bungee cords. There are several limiting factors in using bungee cords. The first is the time and cost of researching and analyzing the correct bungee cord for each specific task. The second is when you have a test requirement to change the mass configuration; the bungee needs to be reconfigured to achieve the same frequency separation between the bungee frequencies and the test article's rigid body frequencies. The third is that the integrity of the bungee cannot be trusted for a critical lift, so a secondary support needs to be configured in case the bungee breaks.

To save time and money a 14,240-lb capacity overhead 3S was designed. This system was designed to keep the frequency separation constant between the 3S and the test article no matter how much the test article's weight changed within 14,240 lbs.

Objective

The objective was to isolate the test article from the effect of being on the ground by using two Firestone airbags (commonly seen as shock absorbers on semi-trucks) as low frequency springs. These airbags were connected to a constant air supply and a regulator to automatically let in air or release air according to how much weight was applied to the airbag. Since a dynamic load can be applied to the airbags during a Structural Mode Interaction Test, linear bearings using lubricated circulating balls were needed to reduce friction to a minimum as a result of the airbags expanding or contracting.

The 3S Design Philosophy and Margin of Safety

It was vital that the 3S be designed so that anyone could use it with minimal instruction and with low risk of damage to the 3S or the test article hanging from it. Two design criteria were identified: positive stops that prevent the airbags from being over inflated and rupturing, and stops which prevent the applied load from resting on un-inflated bags, which could tear the bags. When the bags are not inflated the applied load rests solely on the support structure. This allows the user to lift the test article before or after inflation.

The air regulator was designed to respond as a function of the inflated height of the airbag. As weight is added to the 3S the airbag is compressed so that as the height decreases the regulator will let in more air to maintain the design height. These particular Firestone airbags have a constant spring rate at the design height of 18.5" whether there is 20 - 100 PSIG internal pressure. The maximum allowable internal pressure for each airbag is 120 PSIG. The rated working load is 100 PSIG which allows for a dynamic positive margin of safety. The only way the airbags could register more than 120 PSIG is if a load greater than 17,200 lbs was applied to the 3S.

Figure 1 describes the characteristics of the 14,240-lb 3S referencing a Pro Engineer solid model (note: the second airbag cannot be seen from this angle). The structure is designed with a margin of safety of 3 to adhere to critical lift rules. The airbags have a margin of safety of 4. The 3S was fabricated in the NASA DFRC Machine and Sheet shops. Figure 2 shows a picture of the actual hardware.

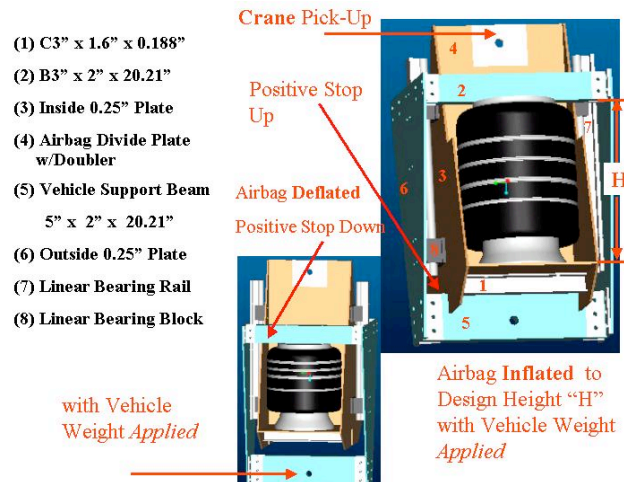


Figure 1. Pro Engineer model of 14,240-lb 3S.



Figure 2. 14,240-lb 3S Hardware.

Status/Plans

The UCAV project has been the main customer for the 14,240-lb 3S so far with 2 GVTs and 3 SMI tests.

Contact:

Starr Ginn, DFRC, RS, starr.ginn@nasa.gov

HXRV3 – Horizontal Tail Ground Vibration Test Results

Summary

The Hyper-X Research Vehicle (HXRV) ship two and ship three have undergone some minor structural modifications compared to ship one. The control horn material was changed from aluminum to steel and slippage was constrained with the addition of keyed locks. The control linkage stiffness directly affected the horizontal tail “rigid” pitch mode shapes which define the predicted critical flutter mechanism. A static compliance test was performed on ship two, to validate the static structure analytical model. When the static structure model was updated and then a follow on structural dynamic analysis was performed, the data showed that the HXRV horizontal tail pitch frequencies dropped due to the linkage modification, see Table 1 under “Analytical FEM After Compliance Test Model Updates” compared to “GVT Ship 1.” A ground vibration test (GVT) was then performed to show that horizontal tail pitch frequencies did not decrease due to an increase in stiffness but rather the frequencies increased. The GVT Ship 3 results showed the use of static compliance test data for dynamic analytical FEM updates is objectionable.

Table 1. Frequency Comparisons.

Modes	Analytical FEM BEFORE Compliance Test Model Updates (hxr090299)	GVT Ship 1	Analytical FEM AFTER Compliance Test Model Updates	GVT Ship 3
1 Horizontal Tail Pitch-Sym	37.54 Hz	40.0	30.5	43.52
2 Horizontal Tail Pitch-Anti-Sym	38.45 Hz	41.9	----	42.68
3 Horizontal Tail Pitch-Sym, Fuselage 1 st Bending-Sym	44.14 Hz	46.6	----	38.83

Objective

An updated ground vibration test (GVT) on the horizontal tails of the HXRV was required to obtain measured data that was used to confirm analytical predictions of aeroelastic stability. The objective was to measure the frequency, modal damping and mode shape of the horizontal tail modes. **Note:** With ship two being so close to flight and already mated to the stack, ship three was tested instead. Ship three has the same actuator linkage modification as ship two, see Figure 1 for modification location, and should give a reasonable estimate of where the horizontal tail pitch modes are.

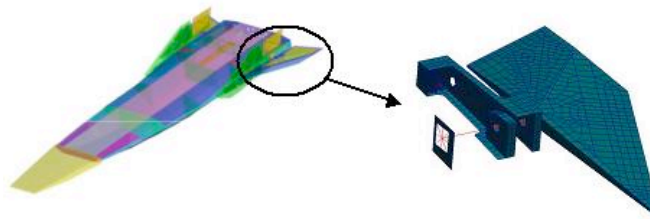


Figure 1. Left- HXRV Dynamic Model. Right HXRV Horizontal Tail Dynamic Model.

Aircraft Configuration and GVT Setup

A soft support system simulates, as closely as practical, the free-flight configuration of the aircraft and acts to isolate the rigid-body modes from the aircraft's elastic-structural modes. For this HXRV horizontal tail test a soft support system was *not* used since the target horizontal tail pitch modes are largely independent of fuselage constraints. One 50-lb shaker was vertically attached to each horizontal tail, Figure 2. A burst random force of 3 lbs RMS was used to excite each horizontal tail.

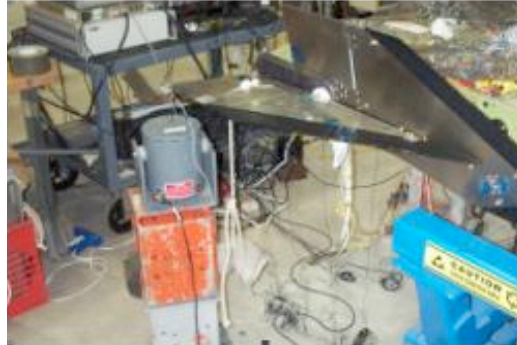


Figure 2. GVT Setup.

Results

After many tests, the cleanest data and clearest mode shapes came from test #38. To identify the proper mode shapes for all of the frequencies recorded, we had to distribute the accelerometers to the main structures of the assembly. It was clear when trying to interpret previous tests that repeated mode shapes meant we were not measuring the correct degrees of freedom. To identify the “real” symmetric and anti-symmetric horizontal tail mode shapes versus the fuselage motion and clamshell motion, we populated the fuselage and clamshell as well as the horizontal tails. Another major contribution to the success of this test was the suggestion to tighten down the control horn upper nut and aft attach point on the actuator as well as actuate or exercise the control surfaces (horizontal tails). After this task was complete (31 tests of trouble shooting later) all of our data cleaned up to an acceptable state. Besides the horizontal tail rotation modes increasing in frequency due to the stiffness increase, the order of the horizontal tail rotation modes switched, Table 1 “GVT Ship 3” data.

Status/Plans

All GVT data was evaluated and the flutter analysis completed. Flight test is scheduled for March 2004.

Contact:

Starr Ginn, DFRC, RS, starr.ginn@nasa.gov
Natalie Spivey, DFRC, RS, 661-276-2790
Roger Truax, DFRC, RS, 661-276-2230

Mode Matching Technique for the Finite Element X-Plane Pylon Models

Summary

The X-Plane Pylon is a welded steel construction, which attaches to the standard B-52H weapons pylon hard points on the right wing and is designed to accommodate vehicles with gross weights up to 25,000 lbs. For the safety of the pylon captive carry flights on the B-52H, an equivalent finite element model of the pylon needs to be created and a flutter analysis performed with this equivalent pylon model mated to the B-52H.

Objective

The objective was to create an equivalent pylon model which would be simple enough to integrate with the beam-stick model of the B-52H (see Figure 1), yet detailed enough to match the reality of the pylon's mode shapes and frequencies.

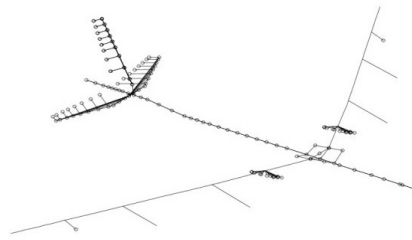


Figure 1. B-52H Beam-Stick FEM.

Approach

The mode matching technique used was a series of optimizations to match the mass and stiffness properties of the equivalent beam model to those of a detailed finite element model (FEM). Once the structural dynamic characteristics of the equivalent model matched the detailed model, a ground vibration test (GVT) was performed to measure the frequency and mode shape of the pylon's primary structural modes. After the GVT, another series of optimizations using the mode matching technique was performed to match the mass and stiffness properties of the analytical equivalent beam model to GVT data.

Results

The equivalent beam pylon model that resulted from this analysis is on the same order of model complexity as that of the B-52H (see Table 1), which makes combining them a mathematical possibility.

		<u># of Nodes</u>	<u># of Elements</u>
B-52H Mother Ship		232	336
X-Plane Pylon	Equivalent Beam	30	77
	Detailed FEM	8941	12038

Table 1. Complexity of the Finite Element Models.

The first series of structural dynamic optimizations, which matched the mass and stiffness properties of the equivalent model to those of a detailed FEM, are seen in Table 2 and Figures 3 and 4. Both models assumed a rigid boundary condition at the connection points where the pylon mates with the B-52H. The optimization took into account 279 mass design variables and 155 stiffness design variables.

Mode	Equivalent Beam		Detailed FEM	% Error
	MAC	Freq. (Hz)	Freq. (Hz)	
Lateral Bending	98.70	34.05	34.05	0.0
Vertical Bending	93.03	46.69	46.69	0.0

Table 2. Equivalent Beam vs. Detailed FEM Comparisons.

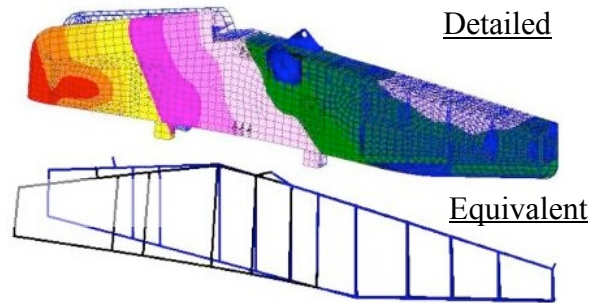


Figure 2. Pylon Lateral Bending 34.05 Hz.

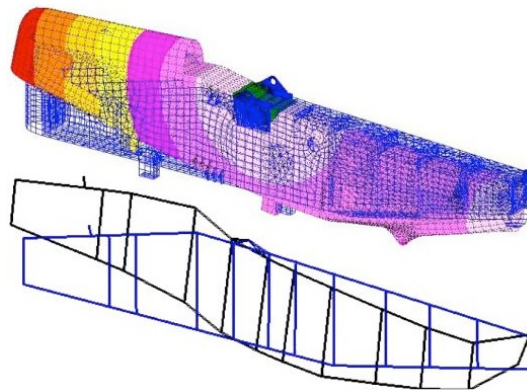


Figure 3. Pylon Vertical Bending 46.69 Hz.

The second mode matching optimization of the equivalent beam model using GVT data showed a change in modes with a pendulum mode appearing, as seen in Table 3 and Figures 4 and 5. The mode change is due to the reality of the non-rigid connections between the B-52H and the pylon.

Mode	Equivalent Beam		GVT Data	% Error
	MAC	Freq. (Hz)	Freq. (Hz)	
Pendulum	98.47	15.56	15.45	0.68
1 st Lateral Bending	97.23	34.70	35.21	-1.44

Table 3. Equivalent Beam vs. GVT Data Comparisons.

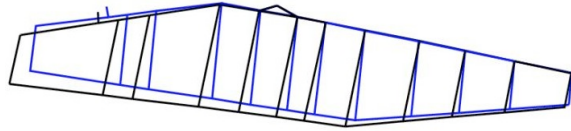


Figure 4. Pylon Pendulum 15.56 Hz.

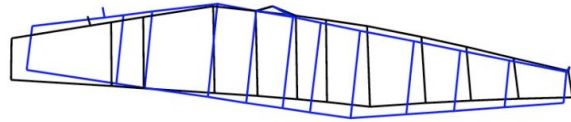


Figure 5. Pylon 1st Lateral Bending 34.70 Hz.

Status/Plans

The aft part of the pylon is currently being modified with an addition of a mortar assembly which will house the drogue chute for the Drogue Chute Test Fixture and the X-37; additional analytical model updates and mode matching will need to be done to include these changes.

Contact

Natalie Spivey, NASA Dryden, Code RS at 661-276-2790

Dr. Chan-gi Pak, NASA Dryden, Code RS at 661-276-5698

Equivalent Beam Modeling of X-43A Stack (Ship 2) Using Mode Matching Techniques

Summary

The X-43A program seeks to demonstrate airframe-integrated, “air-breathing” engine technologies that have potential to increase payload capacity for future vehicles, including hypersonic aircraft and reusable space launchers. A Pegasus rocket booster referred to as the Hyper-X Launch Vehicle (HXLV) lifts the Hyper-X Research Vehicle (HXRV) to its operating altitude, but first it is carried to the launch altitude of the X-43A stack under the wing of a B-52B aircraft. For the safety of the B-52B captive carry flight, structural dynamics Finite Element Models (FEMs) of the B-52B and X-43A stack should be combined and the aeroelastic stability of the combined FEMs will be analyzed prior to flight.

Objective

The objective was to create an equivalent X-43A stack (ship 2) FEM which would be simple enough to integrate with the beam-stick FEM of the B-52B (see Figure 1 and Table 1), yet detailed enough to match the reality of the X-43A stack’s mode shapes and frequencies. The detailed X-43A stack FEM when combined with the B-52B beam-stick FEM produces a huge unbalance in the number of nodes between the two models and causes numerical difficulties during aeroelastic stability analysis. On the other hand, the simple beam X-43A stack FEM (ship 1) created by Orbital Sciences Corporation poorly matches the structural dynamic characteristics of the detailed FEM. This inaccurate simple beam FEM when mated to the B-52B for flutter analysis would produce unreliable flutter results. Therefore, with numerical difficulties with using the detailed FEM in the aeroelastic stability analysis and inaccurate results using the simple beam model necessitate creating an equivalent beam model for the X-43A stack, which would be more efficient than the full detailed model and more accurate than the simple beam model.

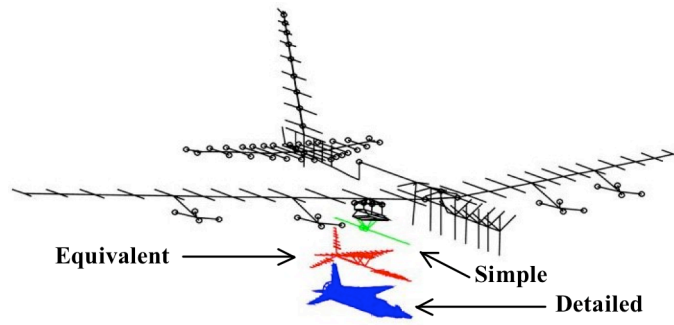


Figure 1. B-52B Beam-Stick FEM w/ Different X-43A Stack FEMs.

		<u># of Nodes</u>
B-52B Beam-Stick FEM		375
X-43A Stack	Simple Beam (ship 1)	69
	Equivalent Beam (ship 2)	165
	Detailed FEM (ship2)	20,130

Table 1. Complexity of the Finite Element Models.

Approach

For this analysis, the mode matching technique used was a series of optimizations, which minimized the discrepancies in frequencies and mode shapes between the X-43A stack’s detailed FEM and the

equivalent beam FEM. Three optimization steps were used: the mass properties were set, the mass matrix was orthogonalized, and then the natural frequencies and mode shapes were matched. See Figure 2 for a diagram of this process. The design variables for the optimization can include structural sizing information (thickness or area of finite elements), concentrated masses, and material properties (density, Young's modulus and spring constants).

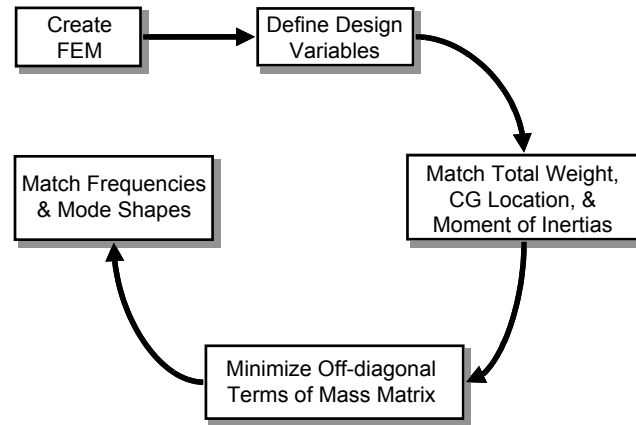


Figure 2. Diagram of Mode Matching Process.

Initially matching the entire equivalent X-43A stack FEM would make it terribly difficult to find reasonable starting conditions, so the X-43A stack was divided into four components: the three tail fins of the HXLV, the HXLV wings, the HXRv with the HXRv adapter and ballast avionics module (BAM), and the HXLV fuselage. The starting point configuration for each stack component was derived from the corresponding segment of the detailed FEM and each component was fully constrained at the nodes where it would connect to the rest of the model. The four components of the stack were matched separately then assembled into the full equivalent beam model.

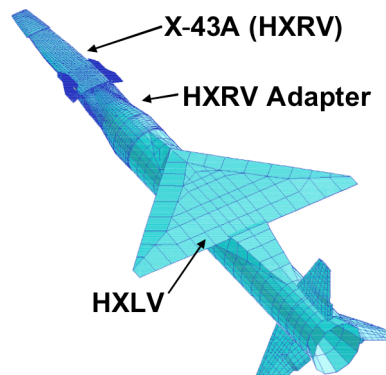


Figure 3. X-43A Stack Detailed FEM.

Results:

The X-43A stack equivalent beam model that resulted from this mode matching process is on the same order of model complexity as that of the B-52B beam stick model (see Table 1), which makes combining the two FEMs a mathematical possibility.

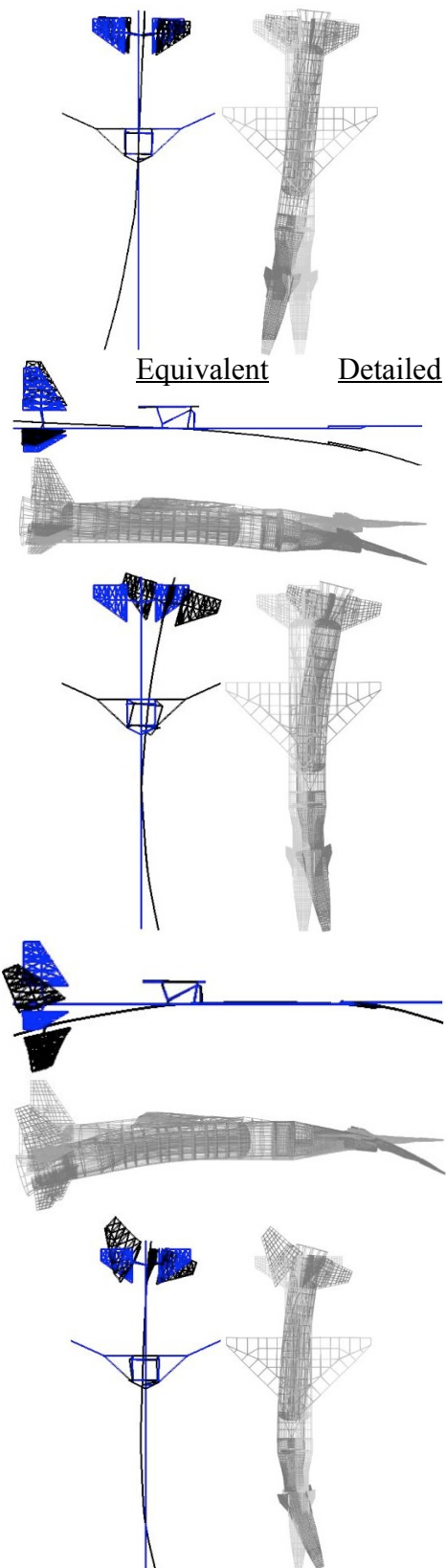
For each stack component the mode matching process was done; however, the number of modes matched varied depending on the number of frequencies below 20 Hz and the ease with which the mode shapes of a particular component could be matched.

Once each stack component was matched to satisfaction, then full equivalent beam model was assembled. The detailed and equivalent models were fully constrained at the same four nodes representing the four attachment points between the X-43A stack and the B-52B adapter. Mass properties were added as design variables at the connection nodes that had been constrained when the components were modeled separately. The design variables defined were the rotational springs attaching the BAM to the HXRV, those attaching the BAM to the HXLV, and the beam properties of the wing supports and HXLV fin supports. The support structure of the wings and fins proved to be the key to matching the full model.

The frequency results for the first five modes of all three models are listed in Table 2. The simple beam model does NOT accurately represent any of the detailed model's natural frequencies, but the equivalent beam model matches the first five frequencies with 0% error. To assess the agreement of mode shapes between the detailed FEM and the equivalent beam FEM, the Modal Assurance Criterion (MAC) was calculated for each mode. The result was on a scale of 0 to 100, with 100 being perfect agreement. The MAC values are also found in Table 2 and the mode shapes are found in Figure 4. The third and fifth modes were the hardest to match because both were highly sensitive to the flexibility of the wing support structure. Further improvement of the mode shapes is possible but computationally expensive. The higher the complexity of the model, the longer the optimization takes. As well, the goal of this model was to be as simple as possible.

<u>Mode</u>	<u>Simple Beam</u> (ship 1)	<u>Equivalent FEM</u> (ship 2)		<u>Detailed FEM</u> (ship 2)
	Freq. (Hz)	MAC	Freq. (Hz)	Freq. (Hz)
Yawing	4.18	89.06	3.65	3.65
Pitching	7.53	96.99	4.42	4.42
1st Lateral Bending	15.66	96.87	6.42	6.42
1st Vertical Bending	25.46	98.70	8.75	8.75
2nd Lateral Bending	28.33	83.43	11.69	11.69

Table 2. Different FEMs Frequency Comparisons.



Mode 1
Yawing 3.65 Hz

Mode 2
Pitching 4.42 Hz

Mode 3
1st Lateral Bending 6.42 Hz

Mode 4
1st Vertical Bending 8.75 Hz

Mode 5
2nd Lateral Bending 11.69 Hz

Figure 4. Mode Shape Comparasions.

Status/Plans

The flutter analysis for the X-43A (ship 2) captive carry flight has been completed using this equivalent beam model mated to the B-52B beam-stick model. The Hyper-X project is currently scheduled for a spring 2004 flight.

Contact

Natalie Spivey, NASA Dryden, Code RS at 661-276-2790

Dr. Chan-gi Pak, NASA Dryden, Code RS at 661-276-5698

X-Plane Pylon and B-52H Ground Vibration Test

Summary

The X-Plane Pylon is a welded steel construction, which attaches to the standard B-52H weapons pylon hard points on the right wing and is designed to accommodate vehicles with gross weights up to 25,000 lbs. Ground vibration testing (GVT) and a flutter analysis are required to quantify the pylon's structural modes, frequencies and aeroelastic stability before the pylon's captive carry flights.

Objective

The objective was to measure the frequency, modal damping and mode shape of the pylon's primary structural modes in the configuration for the captive carry pylon flights. GVT data will be used to better understand the stiffness characteristics between the B-52H and pylon connection points. The pylon analytical model will be updated with GVT results and then the updated analytical model will be used for the flutter analysis.

GVT Configuration

The pylon was in flight configuration and the B-52H was fueled with 100,000 lbs of fuel distributed according to the pylon's flight fuel configuration. The B-52H was stabilized on 19 jacks to create a rigid wing environment and the wingtip gear was tied down to cement blocks as seen in Figure 1. This rigid environment allowed the structural dynamics test team to clearly identify the pylon modes of interest and minimize the number of B-52H modes. There were a total of 103 accelerometers mounted to the pylon and B-52H. One 50-pound shaker was suspended from a crane and was attached to the lower, right corner of the pylon's first bulkhead as seen in Figure 2. The pylon was horizontally excited with burst random inputs at three various force levels.

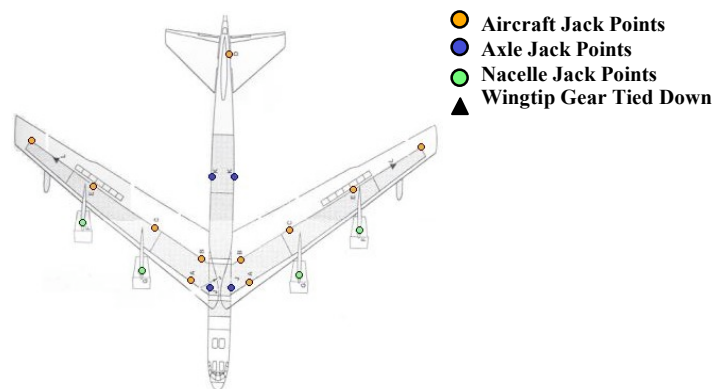


Figure 1. B-52H Jacking Configuration.



Figure 2. X-Plane Pylon GVT Setup w/ Suspended Shaker.

Results

The burst random excitation at a force level of 4.4 RMS (lbs) was curve fit using a polyreference curve fit technique; frequency and mode shape results are shown in Table 1, Figures 3 and 4. GVT data identified the pylon pendulum mode due to the reality of the non-rigid connections between the B-52H and the pylon. The analytical model prior to GVT updates assumed totally rigid connections between the B-52H and the pylon. However, after the analytical pylon model was updated with GVT results the pendulum mode surfaces and the error was dramatically reduced.

<u>Mode</u>	<u>Original Analytical Freq (Hz)</u>	<u>GVT Freq (Hz)</u>	<u>% Error</u>	<u>Updated Analytical Freq (Hz)</u>	<u>% Error</u>
Pendulum	---	15.45	100.0	15.55	0.68
1st Bending	34.05	35.21	3.41	34.7	-1.44

Table 1. Analytical vs. GVT Frequency Comparisons.

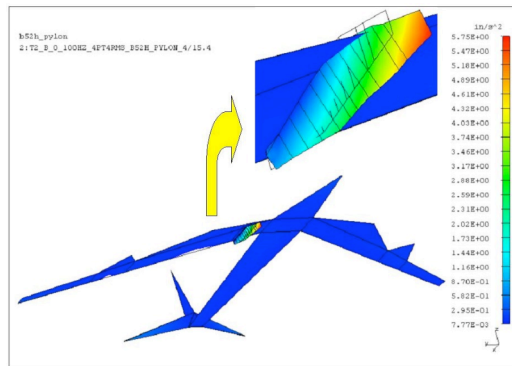


Figure 3. Pylon Pendulum 15.4 Hz.

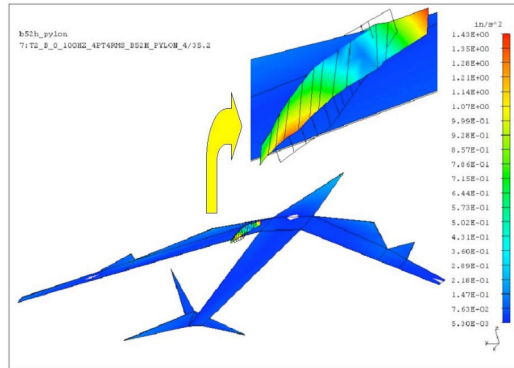


Figure 4. Pylon 1st Bending 35.21 Hz.

Status/Plans

Analytical model updates are completed and the pylon flutter analysis is in work. The pylon captive carry flights will begin in the late spring of 2004 after all structural analyses and pylon checkouts are completed.

Contact

Natalie Spivey, NASA Dryden, Code RS at 661-276-2790

Starr Ginn, NASA Dryden, Code RS at 661-276-3434

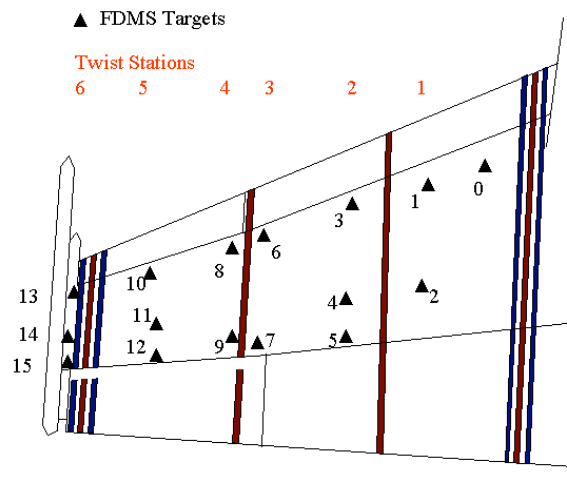
Roger Truax, NASA Dryden, Code RS at 661-276-2230

AAW Twist Model Development

Summary

The Active Aerorelastic Wing (AAW) Twist Model was designed to provide accurate twist predictions at six stations across the span of the AAW aircraft left wing. Though not required for AAW Phase 2 control laws, a reliable twist model is necessary to gain a deeper understanding of the twist developed. Other benefits include evaluation of control design before flight, insight into aircraft performance uncertainties, and assistance with computational fluid dynamic and aeroelastic issues.

The left wing of the AAW aircraft is instrumented with 16 light emitting diode (LED) targets, which relay deflection signals to an optical receiver in the pod just aft of the cockpit. Absolute angle of twist was calculated from the target outputs and served as the independent signal to be predicted. Illustrated below is the AAW left wing where FDMS targets and subsequent twist stations are located.



FDMS Target and Twist Station Locations.

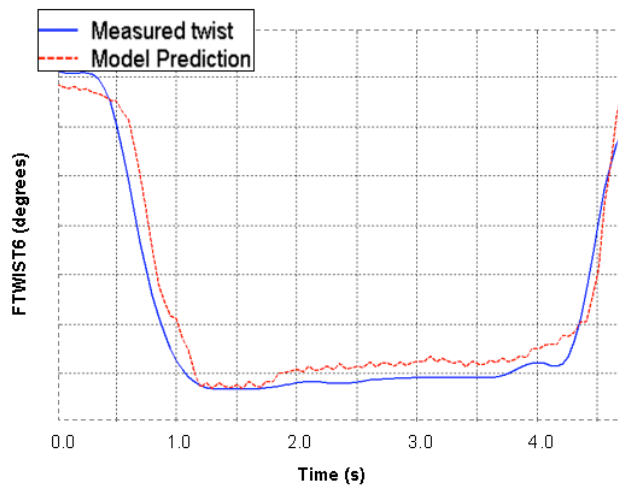
Approach

Hundreds of maneuvers from the primary flight conditions of Phase 1 were collected and conditioned before incorporation into the twist model. Maneuvers to derive the model included surface doublets, rolls, rolling pullouts, wind up turns and push-over-pull-ups. After data from these maneuvers was gathered, processing techniques were used to further reduce the information. Filling signal dropouts, time synchronization, spike removal, signal filtering and other steps were taken to develop suitable files with which an in-house tool, modified to derive twist equations, was utilized.

In-house Equation Derivation (EQDE) software was used to determine influence coefficients for specific aircraft state variables and control surface positions. The technique uses multiple linear regression with either user defined input parameters or an exhaustive search to determine the most efficient set of parameter combinations. Both methods were used in determination of the final parameters. Approximately 85% of the maneuvers were used to derive the model with the remaining 15% used for validation.

Results and Analysis

Models of the four outermost twist stations (FTWIST3, FTWIST4, FTWIST5, and FTWIST6) have been produced for the primary flight conditions. Plotted below is a typical 360° roll at 47% stick, flight condition Mach .90 at 10,000 ft. The graph shows wing tip twist (FTWIST6) measured and predicted. The roll shown is a validation maneuver, which was not used in the model generation and serves as an independent check of the overall prediction.



360° Roll, Wing Tip Twist.

Results have shown a linear precise relationship between the measured twist and aircraft states and surface positions a majority of the time, though there are a few discrepancies. These trends are likely due to friction, Mach effects, nonlinear control surface effectiveness, buffet, control surface aerodynamic interaction, and may possibly be corrected. Other brief observations include overall superior results at subsonic flight conditions and a substantial deficiency in FTWIST4 target data creating considerable error at that station.

Future Work

Twist model results have recently been implemented into the AAW simulator where further evaluation of the model may be achieved through Phase 2 flights. Other work includes quantifying results and investigating benefits of a neural net to better predict twist in non-linear cases.

Point of Contact

Andrew Lizotte
NASA Dryden Flight Research Center
(661) 276-2077

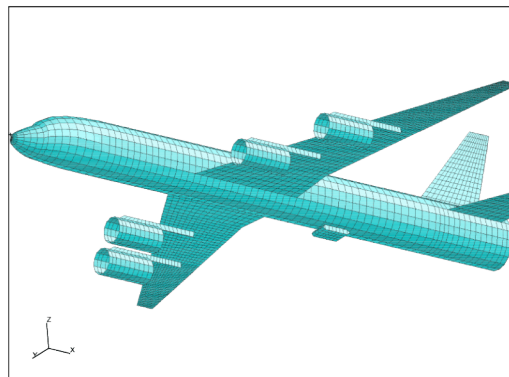
DC-8/Lightweight Rain Radiometer Dynamic and Flutter Modeling

Summary

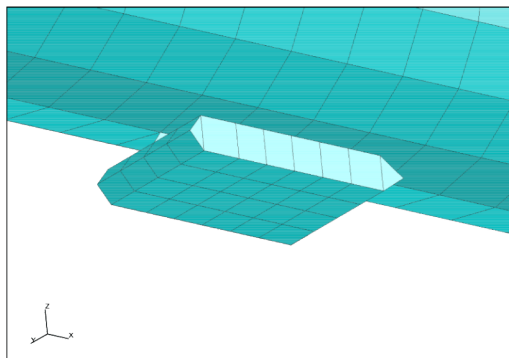
External installation of the relatively large lightweight Rain Radiometer (LRR) to the Airborne Sciences DC-8 raised a concern as to its aeroelastic stability during future flight. A Finite Element Model (FEM) of the DC-8 and LRR configuration was used for structural dynamics and flutter analyses. After several iterations of refining the structural dynamic connection details, the critical flutter was predicted to occur outside the 20% safety margin of the DC-8 flight envelope.

Approach

A detailed stress FEM of the LRR was received from Goddard Space Flight Center. This was to be used for structural dynamics analysis with NASTRAN code. An assumption was made that the much more massive DC-8 would not have aeroelastic coupling with the boxlike LRR mounted under the DC-8 fuselage near its wing box. However, upstream and surrounding aerodynamics of the LRR would be modeled with a representation of the DC-8's external geometry. Without an existing FEM of the DC-8, a simple one was created using rigid elements, total mass and mass moment of inertia. Unsteady aerodynamic paneling of the DC-8 and LRR was generated using available drawings and PATRAN.

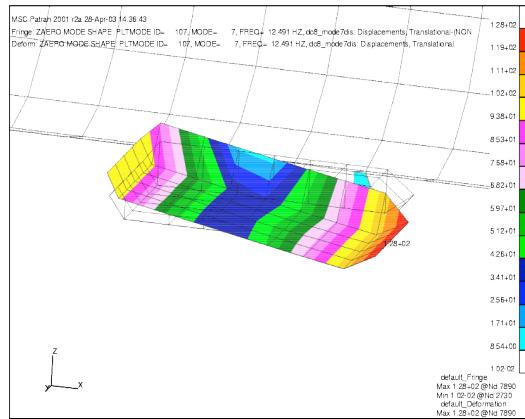


DC-8/LRR Unsteady Aerodynamic Paneling.



LRR Close-up.

The LRR FEM dynamic mode shapes were splined (interpolated) to the unsteady aerodynamic paneling.

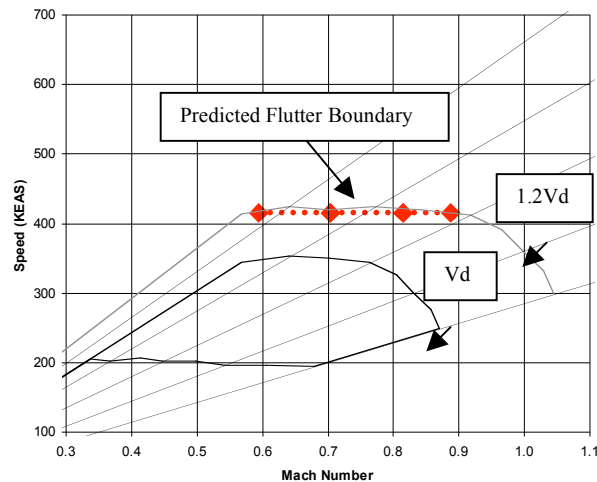


LRR First Elastic Dynamic (Rigid Pitch, 12.49 Hz) and Critical Flutter Mode.

Flutter analysis was performed using the newly obtained ZAERO code and linear theory. Six DC-8 rigid body modes and twenty LRR elastic modes were included. Matched point (real atmosphere) flutter solutions at Mach numbers of 0.6, 0.7, 0.8 and 0.9 were obtained. A typical structural damping of 0.02 g's was assumed for the actual flutter speed crossing.

Results

The structural mode that led to the predicted flutter instability was an LRR rigid pitch at 12.49 Hz. No coupling with other modes was observed. The instability occurred outside of a 20% margin of the flight envelope.



Contact

Chan-gi Pak, DFRC, RS (661) 276-5698
 chan-gi.pak@dfrc.nasa.gov
 Roger Truax, DFRC, RS (661) 276-2230
 roger.truax@dfrc.nasa.gov

Generation of B-52H Mother Ship Dynamic and Flutter Models

Summary

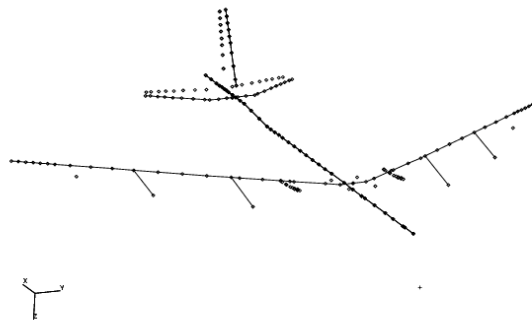
As an eventual replacement mother ship for the aging B-52B-008, the relatively new B-52H-025 was modeled for use in structural dynamics and flutter analyses. The dynamics model used by Boeing, Wichita for Air Force fleet use has been modified and expanded to represent the NASA Dryden aircraft. A detailed flutter model was generated from the outer moldline dimensions.



Dryden's New B-52H-025 in Clean Configured Flight.

Approach

The symmetric and anti-symmetric half aircraft dynamics “stick” model obtained from Boeing had to be mirrored to a full tip-to-tip model for asymmetric analyses of the right wing store configurations. These are typical of Dryden's mother ship operations when carrying vehicles such as the X-37, X-38 and X-43A and for future programs as well. This would be accomplished by mirroring the NASTRAN model elements, coordinate systems and mass matrices using PATRAN. To bypass difficulties with mirroring the centerline, its properties were halved, elements doubled and then connected together with rigid elements. Dynamics analysis results of half and full aircraft models were compared to verify that the model stiffness and mass had not changed.



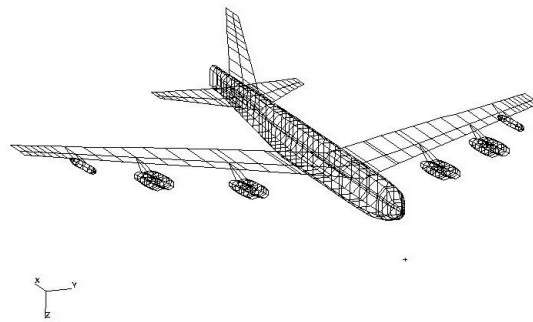
Dynamics “stick” model.

Another major task was to remove the many Air Force non-structural mass items from the model that were taken out of the aircraft during the de-militarization effort for conversion to the NASA

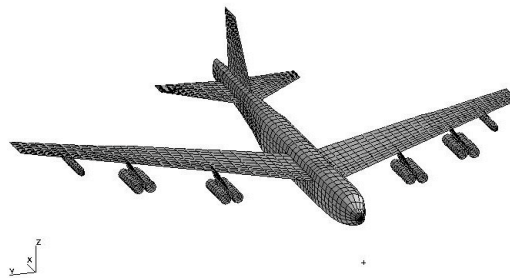
configuration. Many items were identified but several were not. An iterative process was used to refine the mass distribution to match weight and balance records of the aircraft while at Edwards.

To generate the unsteady aerodynamics model, the outer mold line of the aircraft would be needed. Fortunately, Edwards Air Force Base structural dynamics engineers had performed a 3-dimensional laser scan of a typical B-52H aircraft that resulted in a Pro-Engineer model. This was used for the ZAERO code unsteady aerodynamics model paneling and to generate mold line elements to better visualize the dynamics “stick” model. The later consisted of massless and zero stiffness plates rigidly attached to the beam elements of the stick dynamics model. This doesn’t affect the dynamics results but greatly assists in the identification of the numerous, and complicated, B-52 modes.

With the basic aircraft modeling completed, structural dynamics and then flutter analyses were performed to establish baseline results. These results will be compared to those of any future store (under the right wing) to determine any restrictions to the flight envelope for those flights.



Dynamics Model with Visualization Elements.



Unsteady Aerodynamics Flutter Model.

Contact

Chan-gi Pak, DFRC, RS (661) 276-5698

chan-gi.pak@dfrc.nasa.gov

Roger Truax, DFRC, RS (661) 276-2230

roger.truax@dfrc.nasa.gov

X-43A Wing Control Horn Dynamic Modeling, Verification and Aeroelastic Effects

Summary

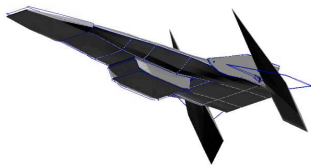
Modifications were made to increase the X-43A wing control horn stiffness of ships two and three over that of ship one. Subsequent wing compliance test results that indicated increased rotation per unit torque (less stiffness) were opposite of expectations. The wing pitch stiffness needed to be accurately modeled for flight predictions of aeroelastic stability. A limited Ground Vibration Test (GVT) performed on flight hardware generated more favorable results that were used to modify the structural dynamics model. Aeroelastic stability analyses that followed predicted less margin of safety than with the compliance test results but the instability remained well outside the flight envelope.

Background

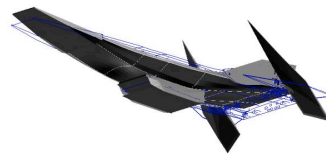
The wing control horn modification specifically involved a change of material from aluminum to steel and a new keyed lock to prevent slippage. This would increase its linkage stiffness that directly controls the wing pitch modes. However, the compliance test resulted in less stiffness than the ship one configuration. These compliance test results were initially used for modification of the structural dynamics model stiffness and thus generated a 20% drop in the frequency of X-43A's first elastic mode; symmetric wing pitch. With this mode being involved in the vehicle's critical flutter mechanism and the uncertainty of the compliance test results, the question was raised as to what are the frequencies of the critical modes and what would be the effect on aeroelastic stability.

Approach

A GVT would resolve the above question. It has traditionally been used to verify structural dynamics modeling of flight hardware. The target modes to measure would be symmetric and anti-symmetric wing pitch as well as the fuselage first bending mode that is actually dominated by symmetric wing pitch as well. It is the frequency separation of the symmetric wing pitch and fuselage first bending modes that delays their coupling to form the critical aeroelastic instability.



Symmetric Wing Pitch.



Symmetric Fuselage 1st Bend.

There was hope that a freely floating vehicle GVT with its much higher costs, duration and effort could be avoided. Fortunately, the Test Analytical Model (TAM) target mode shapes and frequencies of the vehicle rigidly attached to its cradle support structure had very little change from a free configuration. The rigid supports were at or very near modal node lines of zero motion. The TAM would also have missing flight hardware not present in the GVT. These would be put back after the TAM was correlated to GVT mode shapes and frequencies. These hardware mass items were not related to the target mode stiffness of the wing linkage.

Due to vehicle availability, the GVT was performed on X-43A ship three which had the same wing actuator hardware modification as ship two, the vehicle in question. The actual GVT configuration did

not have the fuselage upper panel attached. This was not anticipated but was not a concern since the fuselage modeling had been verified by a previous freely floating GVT on sister ship one. Even though the third target mode had some fuselage bending present, it was the unrelated wing pitch motion that was of significance.

Frequencies of the target modes from the GVT had been measured and had already been high enough to confirm their increased stiffness from the control horn modification. But the TAM still had to have its control horn modified to match those higher GVT frequency results. Attempts to stiffen the control horn NASTRAN CBAR element itself resulted in essentially no frequency increase. Then the pushrod, a CROD element, from the actuator to the control horn was used but an asymptotic limit (infinitely stiff) was found before reaching GVT frequencies. Finally, a CBAR element was substituted for the CROD element and was successful in attaining near GVT frequencies although at its own infinitely stiff limit. With this TAM correlation completed, the test constraints were released and hardware masses re-added to constitute the free flight configuration.



Artist's Concept of the X-43A in Free Flight.

Results

The free-free structural dynamics model results confirmed the estimates of higher wing pitch frequencies that were consistent with stiffer control horns. The frequency separation between the critical flutter modes was increased a little but the order of those modes had switched; the previous lower frequency mode was now higher and had opposite wing-fuselage phasing than before. This could mean that the ship one critical flutter mechanisms may no longer apply to ships two and three. New flutter analyses were recommended for ships two and three and were performed at Boeing, Huntington Beach. The predicted flutter instabilities had changed from previous analyses but, with a sigh of relief, remained well outside the flight envelope.

Contact

Roger Truax, DFRC, RS (661) 276-2230

roger.truax@dfrc.nasa.gov

Aeroservoelastic Stability Analysis of X-43A Stack

Summary

In an attempt to predict the first flight instability of the X-43A stack, an investigation was performed using linear aeroelastic and aeroservoelastic analyses. Anti-symmetric low frequency motions, such as rolling and yawing oscillations, that were evident just prior to its loss of control necessitated more realistic surface representation in the aerodynamic paneling. Additional modeling features that were employed here, but not previously utilized, were cylindrical body aerodynamic paneling, the mean flow effect, and atmospheric matched point solutions. The oscillatory commands to the stack fins, before the failure, would press the need to include the stack flight control laws for an aeroservoelastic analysis.

The failure mode for the first X-43A stack flight was successfully captured with the linear flutter analysis. When the stack flight control laws were implemented, for the aeroservoelastic stability analysis, the flutter velocity was decreased drastically and approached that observed in actual flight. This flutter speed prediction can be enhanced when the flight control system and/or aerodynamic nonlinearities are included in the analysis.

Approach

The detailed aerodynamic model, including 6076 box divisions, can be seen in Figure 1. The slender body effects of the HXLV and HXR/V are included in this aerodynamic model. Six rigid as well as 60 flexible structural dynamics modes computed from the MSC/NASTRAN simulation were used for the matched flutter analysis. The g-method in the ZAERO code was selected in the matched flutter analysis. Aerodynamic influence coefficient matrices were generated at 16 reduced frequencies.

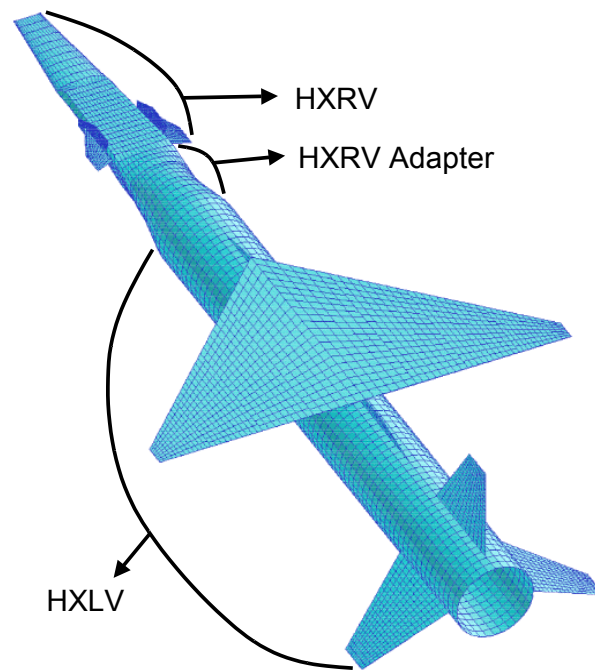


Figure 1. Aerodynamic Model.

Results

The linear aeroservoelastic stability analysis together with the proposed correction factor in Figure 2 can be used for the second and third X-43A stack flights.

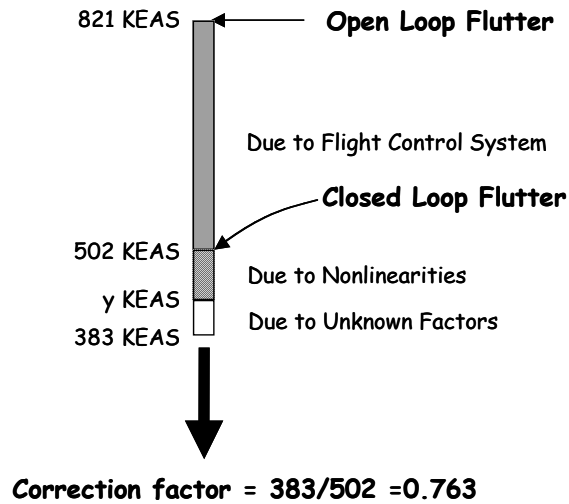


Figure 2. Discrepancies in Flutter Speeds.

Contact

Chan-gi Pak, Structural Dynamics Group, Code RS

Chan-gi.Pak-1@nasa.gov (661) 276-5698

Flight Investigation of Prescribed Simultaneous Independent Surface Excitations (PreSISE) for Real-Time Parameter Identification

Summary

Near real-time stability and control derivative extraction was required to support flight demonstration of Intelligent Flight Control System (IFCS) concepts being developed by NASA, academia, and industry. Traditionally, flight maneuvers were designed and flown to obtain stability and control derivative estimates using a post-flight analysis technique. The IFCS requirement was to be able to modify control laws in real time for an aircraft that has been damaged in flight (due to battle, weather, or a system failure). Prescribed Simultaneous Independent Surface Excitations (PreSISE) were developed and tested in-flight to demonstrate the ability to rapidly obtain estimates of the aircraft stability and control derivatives. During PreSISE maneuvers, all desired control surfaces are excited simultaneously, but at different frequencies, resulting in aircraft motions in all axes.

Objectives

In post-flight analysis, determine

- Accuracy of derivatives estimated from PreSISE
- Length of PreSISE inputs required
- Minimum size of PreSISE inputs required

Approach

PreSISE consisted of stacked sine wave excitations at various frequencies for symmetric canard, symmetric stabilator, differential canard, differential stabilator, aileron, and rudder control surfaces for the highly modified F-15 aircraft shown in Figure 1. Small, medium, and large excitations were tested in 15 second maneuvers at subsonic, transonic, and supersonic speeds. Typical control surface time histories are shown in Figure 2. Flight test data were analyzed using a Dryden-developed industry standard output-error technique known as pEst. Data were also analyzed using an equation error technique known as Fourier Transform Regression (FTR) which was developed to provide on-board real-time derivative estimation.



Figure 1. Modified F-15 aircraft.

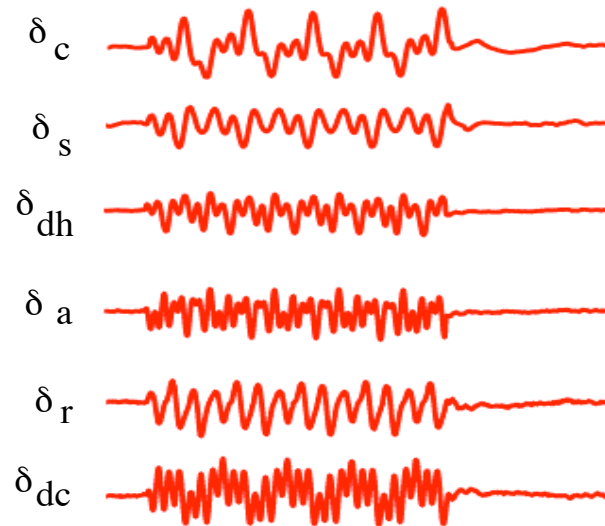


Figure 2. PreSISE time history.

Results

Figure 3 shows results from 9 PreSISE maneuvers at Mach 0.75. At this Mach number, the aircraft is statically unstable. The first set of data are small PreSISE inputs, the second set are medium inputs, and the third set are large inputs. For this derivative, the estimate was the same independent of input size or analysis technique. Typically, the longitudinal derivatives were estimated with good accuracy and, using FTR, converged to a final answer after about 5 seconds of inputs. Some lateral-directional derivatives were not estimated as accurately due to low signal-to-noise. Efforts are currently underway to optimize the inputs for improved derivative estimation accuracy.

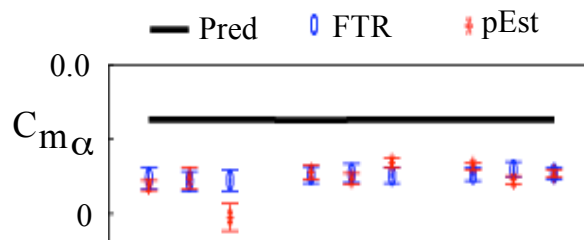


Figure 3. Stability derivative estimates from small, medium, and large PreSISE using FTR and pEst analysis.

Contacts

Tim Moes, DFRC, RA (661) 276-3054
 Mark Smith, DFRC, RA (661) 276-3177
 Gene Morelli, LaRC, (757) 864-4078

Tech Briefs and Patents

NASA Tech Briefs Articles

Michael Thompson, Charles Jorgensen, John Bosworth, Steve Jacobson, Ronald Davidson
Flight Test of an Intelligent Flight-Control System
DRC-001-035

John Burken, Frank Burcham, John Bull
Advances in Thrust-Based Emergency Control of an Airplane
DRC-097-021

Richard Lind
Modeling and Control of Aerothermoelastic Effects
DRC-001-021

David Voracek, Richard Lind, Timothy Doyle, Roger Truax, Starr Potter, Martin Brenner, Leonard Voelker, Lawrence Freudinger, Clifford Sticht
Aerostructures Test Wing
DRC-001-037

Richard Lind, Martin Brenner
Flight-Test Evaluation of Flutter-Prediction Methods
DRC-001-057

Stephen Corda, Michael Vachon
Probe Without Moving Parts Measures Flow Angle
DRC-001-009

Patrick Stoliker, John Carter
Flight Tests of a Ministick Controller in an F/A-18 Airplane
DRC-001-033

Mark Nunnelee
Force-Measuring Clamps
DRC-099-037

Nathan Palumbo, Michael Vachon, David Richwine, Timothy Moes, Gray Creech
Propulsion Flight-Test Fixture
DRC-002-023

Gregory Noffz, Daniel Leiser, Jim Bartlett, Adrienne Lavine
Hot Films on Ceramic Substrates for Measuring Skin Friction
DRC-001-048

Patent

Airforce Shaped Flow Angle Probe
DRC-001-009

REPORT DOCUMENTATION PAGE					Form Approved OMB No. 0704-0188	
<p>The public reporting burden for this collection of information is estimated to average 1 hour per response, including the time for reviewing instructions, searching existing data sources, gathering and maintaining the data needed, and completing and reviewing the collection of information. Send comments regarding this burden estimate or any other aspect of this collection of information, including suggestions for reducing this burden, to Department of Defense, Washington Headquarters Services, Directorate for Information Operations and Reports (0704-0188), 1215 Jefferson Davis Highway, Suite 1204, Arlington, VA 22202-4302. Respondents should be aware that notwithstanding any other provision of law, no person shall be subject to any penalty for failing to comply with a collection of information if it does not display a currently valid OMB control number.</p> <p>PLEASE DO NOT RETURN YOUR FORM TO THE ABOVE ADDRESS.</p>						
1. REPORT DATE (DD-MM-YYYY) 25-07-2005		2. REPORT TYPE Technical Memorandum			3. DATES COVERED (From - To)	
4. TITLE AND SUBTITLE 2003 Research Engineering Annual Report				5a. CONTRACT NUMBER		
				5b. GRANT NUMBER		
				5c. PROGRAM ELEMENT NUMBER		
6. AUTHOR(S) Patrick C. Stoliker, Brad Flick, and Everlyn Cruciani				5d. PROJECT NUMBER		
				5e. TASK NUMBER		
				5f. WORK UNIT NUMBER ES7		
7. PERFORMING ORGANIZATION NAME(S) AND ADDRESS(ES) NASA Dryden Flight Research Center P.O. Box 273 Edwards, California 93523-0273				8. PERFORMING ORGANIZATION REPORT NUMBER H-2582		
9. SPONSORING/MONITORING AGENCY NAME(S) AND ADDRESS(ES) National Aeronautics and Space Administration Washington, DC 20546-0001				10. SPONSORING/MONITOR'S ACRONYM(S) NASA		
				11. SPONSORING/MONITORING REPORT NUMBER NASA/TM-2005-212874		
12. DISTRIBUTION/AVAILABILITY STATEMENT Unclassified -- Unlimited Subject Category 99 Availability: NASA CASI (301) 621-0390 Distribution: Standard						
13. SUPPLEMENTARY NOTES An electronic version can be found at the NASA Dryden Flight Research Center Web site, under Technical Reports.						
14. ABSTRACT Selected research and technology activities at Dryden Flight Research Center are summarized. These activities exemplify the Center's varied and productive research efforts.						
15. SUBJECT TERMS Aerodynamics, Flight, Flight controls, Flight systems, Flight test, Instrumentation, Propulsion, Structures, Structural Dynamics						
16. SECURITY CLASSIFICATION OF:			17. LIMITATION OF ABSTRACT	18. NUMBER OF PAGES	19a. NAME OF RESPONSIBLE PERSON	
a. REPORT	b. ABSTRACT	c. THIS PAGE			STI Help Desk (email: help@sti.nasa.gov)	
U	U	U	UU	98	19b. TELEPHONE NUMBER (Include area code) (301) 621-0390	